JAERI-Data/Code
97-020

EXPERIMENTAL DATA ON CONCRETE SHIELD TRANSMISSION OF QUASI-MONOENERGETIC NEUTRONS GENERATED BY 43-AND 68-MEV PROTONS VIA THE ^{7}Li(p,n) REACTION (JOINT RESEARCH)

June 1997

Noriaki NAKAO*1, Hiroshi NAKASHIMA, Yukio SAKAMOTO
Yoshihiro NAKANE, Shun-ichi TANAKA, Susumu TANAKA
Takashi NAKAMURA*2, Kazuo SHIN*3 and Mamoru BABA*4

日本原子力研究所
Japan Atomic Energy Research Institute

本レポートは，日本原子力研究所が不定期に公刊している研究報告書です。
入手の問合わせは，日本原子力研究所研究情報部研究情報課（〒319-11 茨城県那珂郡東海村）あて，お申し越しください。なお，このほかに財団法人原子力弘済会資料センター（〒319-11 茨城県那珂郡東海村日本原子力研究所内）で複写による実費頒布をおこなっております。

This report is issued irregularly.
Inquiries about availability of the reports should be addressed to Research Information Division, Department of Intellectual Resources, Japan Atomic Energy Research Institute, Tokai-mura, Naka-gun, Ibaraki-ken 319-11, Japan.

編集兼発行　日本原子力研究所
印　　刷　㈱原子力資料サービス

Experimental Data on Concrete Shield Transmission of Quasi-monoenergetic Neutrons Generated by 43-and 68-MeV Protons via the ^{7}Li(p,n) Reaction (Joint Research)

Noriaki NAKAO *1 , Hiroshi NAKASHIMA, Yukio SAKAMOTO
Yoshihiro NAKANE, Shun-ichi TANAKA+ , Susumu TANAKA++
Takashi NAKAMURA*2 , Kazuo SHIN*3 and Mamoru BABA*4

Center for Neutron Science
Tokai Research Establishment
Japan Atomic Energy Research Institute
Tokai-mura, Naka-gun, Ibaraki-ken

(Received May 7, 1997)

The experimental data of neutron transmission through concrete shield of thickness up to 200cm are compiled. The measurements have been conducted by using the quasi-monoenergetic neutron sources of 43- and 68-MeV p-^{7}Li reactions at the TIARA Facility of JAERI. The transmitted neutron energy spectra in the energy region between 10^{-4} eV and the peak neutron energy and reaction rates are given for the five different type detectors; BC 501A scintillation counter, Bonner ball counter, ^{238}U and ^{232}Th fission counters, ^{7}LiF and ^{nat}LiF TLDs, and solid state nuclear track detectors. The neutron dose equivalent behind the shield is also given on the basis of experimental data using a neutron rem counter. All the data in this report are provided numerically for readers' convenience in benchmark calculations.

Keywords: Transmission, Concrete, Shield, Quasi-Monoenergetic Neutron, Neutron Spectrum, Reaction Rate, Neutron Dose Equivalent, Benchmark

---

This research report is the result of the joint study with University of Tokyo, Tohoku University and Kyoto University.
+ Office of Planning
++ Advanced Radiation Technology Center, Takasaki Radiation Chemistry Research Establishment
*1 Former, University of Tokyo, Institute for Nuclear Study
*2 Tohoku University, Cyclotron and Radioisotope Center
*3 Kyoto University
*4 Tohoku University

JAERI－Data/Code 97－020

43及び68MeV陽子の^{7}Li(p, n)反応により発生する準単色中性子を用いたコンクリート遮蔽体透過実験における測定データ
（共同研究）

日本原子力研究所東海研究所中性子科学研究センター
中尾　徳晶[*1]・中島　宏・坂本　幸夫
中根　佳弘・田中　俊一[+]・田中　進[++]
中村　尚司[*2]・秦　和夫[*3]・馬場　護[*4]

（1997年5月7日受理）

原研高崎研の90MeV-AVFサイクロトロン施設において43及び68MeV陽子の^{7}Li(p, n)反応によるビーム状準単色中性子を200㎝厚さまでのコンクリート遮蔽体に入射して行った遮蔽実験データをまとめた。本データは，遮蔽体後面においてBC501Aシンチレーション検出器及びボナーボール検出器により測定した中性子エネルギースペクトルデータ，及び遮蔽体後面または内部においてボナーボール検出器，^{238}U / ^{232}Thの核分裂計数管，^{7}LiF / ^{nat}LiFのTLD，固体飛跡検出器により測定した中性子計数率のほか，遮蔽体後面において中性子レムカウンターにより測定した中性子線量当量についてまとめたものである。本報告書は，ベンチマーク計算に供するため，これらの実験データを数値によって公開した。

本報は，東京大学，東北大学及び京都大学との共同研究の成果である。
東海研究所：〒319-11　茨城県那珂郡東海村白方白根2-4
+ 企画室
++ 放射線高度利用センター
*1 旧 東京大学原子核研究所
*2 東北大学サイクロトロンRIセンター
*3 京都大学
*4 東北大学

Contents

目　　次

1. INTRODUCTION

According to the increase of beam energy and facility number, accelerators are used for a variety of purposes. In high energy accelerator facilities, the shielding of high energy neutrons is of great importance to keep the radiation level of the working area and surrounding environment as low as possible. With the increase of the accelerating beam current and energy, the facilities require more massive concrete shields than before. The shielding design of higher accuracy is inevitable to save the construction cost. The experimental shielding data are, however, very scarce in the energy range above 20 MeV, because the number of shielding experiment facilities for neutrons above 20 MeV are very few and the spectroscopy of higher energy neutrons is not easy.

Meulder et al.[1], Shin et al.[2] and Uwamino et al.[3] measured the energy spectra of neutrons transmitted through various shielding materials using broad spectral neutrons whose maximum energies were about 50 MeV. Ishikawa et al.[4] used quasi-monoenergetic neutron sources generated in a thin Li target by 25- and 35-MeV protons for concrete and iron shielding experiments. In the higher energy range, Moritz et al.[5] measured the leakage neutron spectra outside the concrete shielding in the 500-MeV proton accelerator facility.

A concrete shielding experiment[6] was performed using the p-^{7}Li quasi-monoenergetic neutrons at the 90-MeV AVF cyclotron facility of the TIARA (Takasaki Ion Accelerator for Advanced Radiation Application) in JAERI (Japan Atomic Energy Research Institute). We have already reported the experimental data of iron shielding.[7,8] In the present work, we provide the experimental data of concrete shielding for 40- and 65-MeV neutrons which are practically important for shielding design calculation of high energy accelerator facilities. The data can be used for investigating the accuracy of calculation code and cross section data library.

2. EXPERIMENT

2.1 TIARA facility and experimental set up

The AVF cyclotron facility was completed in 1992. It has an unique neutron beam course named LC-course arranged for the neutron shielding and cross section experiments. The cross sectional view of the LC-course is shown in Fig. 1. An experiment space of 120 cm x 120 cm x 120 cm is prepared inside the 340-cm-thick concrete shielding wall between the accelerator room and the experimental room. The concrete shield of 25 to 200 cm thickness was assembled on a movable stand with 120 cm x 120 cm by 25-cm-thick slabs. The assembly was in contact with the exit of 10.9-cm-diameter collimator located at about 4 m from the ^{7}Li target. This collimator is used as a rotary beam shutter, through which the neutron beam was injected into the shield when the shutter was open, as shown in Fig.1.

The additional iron collimator shown in Fig.2 was used only for measurements with thinner shield, 25- and 50-cm thick concrete, in order to depress the neutron leakage through fillers of iron ball and iron sand or rotary shutter of iron and polyethylene which include low density materials or void. 40- and 80-cm-thick iron collimators used for 43- and 68-MeV p-^{7}Li neutron experiments, respectively, were assembled with 120 cm by 120 cm iron slabs of 20 cm thickness having a cylindrical hole of 10.9 cm diameter. The density and the atomic composition of the concrete shield and the additional iron collimator are given in Table 1. The dimensions of shields and collimators for each experiment are summarized in Table 2.

2.2 Neutron sources

The source neutrons were generated by bombarding 43- and 68-MeV protons on 3.6-mm-thick and 5.2-mm-thick ^{7}Li targets, respectively. The isotopic enrichment of ^{7}Li was 99.9 %. The protons which penetrated the target with the 2-MeV energy loss were bent down toward the beam dump by the clearing magnet and their integrated charge was measured with the current integrator through a Faraday cup for beam current monitoring. The neutrons produced in the forward angle can reach the experimental assembly through the collimator without accompanying protons.

The spectra of quasi-monoenergetic neutron source were measured with a BC501A organic liquid scintillation counter using the time of flight (TOF) method. The measured source neutron energy spectra are shown in Fig.3 and their values are given in Tables 3 and 4.

The absolute flux of source neutrons in the monoenergetic peak per proton beam charge (μC) has been obtained from a proton-recoil-counter-telescope (PRT) measurement[9], to which the

neutron spectra by the TOF method were normalized. The errors of the source neutron peak fluxes by PRT are 3.4 and 3.9 % for 43- and 68-MeV p-Li experiment, respectively. Two fission chambers of ^{238}U and ^{232}Th were placed near the target, and were calibrated to the proton beam current. They were used for monitoring the proton beam current of very low intensity which could not directly be measured due to the dark current. The error of conversion factor of fluence monitor counts to total charges of proton beam is ~3 %. The range of proton currents in this experiment was 0.5 nA to 3 μA.

2.3 Neutron detectors and data analysis

For the shielding experiment, six kinds of detectors were used for the measurement of neutron spectra and reaction rates behind and inside the concrete shields. The detector positions for each experiment are given in Table 2.

2.3.1 BC501A scintillation counter

One of the neutron spectrum measurements in the shielding experiment was performed with the 12.7-cm-diameter x 12.7-cm-long BC501A organic liquid scintillation counter (Bicron Co. Ltd.) coupled to a R4144 photomultiplier (Hamamatsu Photonics. Co. Ltd.). The event-by-event data measured with BC501A were converted to a two-dimensional distribution of pulse-height and rise-time, and the neutron pulse-height distributions were discriminated from the γ-ray pulses. Then they were converted into the neutron energy spectra using the FERDOU[10] unfolding code and the measured response functions.[11] The responses are exemplified in Fig.4 and all numerical data are given in Table 5. The energy calibration of the light output pulses was performed at the zero cross point, the Compton edge of 4.43 MeV γ-rays from a ^{241}Am-Be source and the recoiled proton edge of 40- or 65-MeV monoenergetic neutron peak by using the calibration values in Ref.[11]. The difference of the scaler counts of total output pulses and the number of events recorded in the hard disk was used for the dead time correction. Finally the absolute values of the transmitted spectra are represented as the flux per proton beam charge (μC) which can be estimated from the fluence monitor counts.

2.3.2 Bonner ball counter

A multi-moderator spectrometer, Bonner ball counter, was also used for measurements of neutron spectra and reaction rates behind the concrete shield. It has a spherical polyethylene moderator whose thickness is chosen from 0-, 1.5-, 3.0-, 5.0- and 9.0-cm. In the cases of 100- and 150-cm thick concrete for 68-MeV p-^{7}Li neutrons, 1.5-cm thick moderator covered with 1-mm thick cadmium were used. The thermal neutron detector inserted at the center of the moderator is a 5.08-cm-diameter spherical proportional counter, filled with 10 atm (at 22 °C) ^{3}He gas, made by LND Inc.

The five reaction rates for the five kinds of moderator thickness were unfolded with the SAND-2 code[12] and the response functions given by Uwamino et al.[13] The response functions are shown in Fig. 5 and tabulated in Table 6. Initial guess spectra at each measured position used in the unfolding were obtained from the MORSE[14] calculations with the DLC119/HILO86[15] cross section library. We then obtained the neutron spectra in the energy range from 10^{-4} eV to the peak energy.

2.3.3 Fission counter

The ^{238}U and ^{232}Th fission chambers (Centronic FC480/1000) with 10.1-cm-long x 3.81-cm-diameter active size were used for measuring fission rates behind the concrete shield. The absolute efficiencies were calibrated by a ^{252}Cf spontaneous fission neutron source[16] in JAERI. The measured inverse efficiencies are 1.05 x 10^{3} and 9.86 x 10^{2} barn/cm^{2}/counts (±4 and 3.4 %), respectively. The fission cross sections of ^{238}U and ^{232}Th have been evaluated up to 20 MeV in JENDL-3,[17] based on the measurements by Lisowski et al.[18,19] in the energy region between 20 and 400 MeV. The cross sections are shown in Fig. 6 and the group cross section data are given in Table 7.

2.3.4 Thermoluminescent dosimeter (TLD)

Reaction rates were measured on the beam axis inside the concrete shield using ^{7}LiF and ^{nat}LiF TLDs (Harshaw Co. Ltd.) of 1 x 1 x 6 mm^3. Thermoluminescence was converted to the absolute dose in TLD using a calibration factor determined with a ^{60}Co γ-ray source within the uncertainty less than 3 %. The neutron energy responses were calculated by a code developed by Hashikura et al. on the basis of the KERMA calculation.[20] The calculated neutron energy responses are shown in Fig. 7 and tabulated in Table 8.

2.3.5 Solid state nuclear track detector (SSNTD)

Reaction rates inside the shield were also measured using solid state nuclear track detectors which were manufactured by Nagase Landauer Ltd. The composition of the detector is Allyl diglycol carbonate which is the same as that of CR-39. The detector is a rectangular solid of 10-mm x 5-mm and 1-mm-thick on which a 1-mm thick polyethylene radiator is contacted. After the exposed detectors were etched chemically, the etch pits on the detectors were counted through an optical microscope of 400 times magnifications. The detector response was calculated by a newly-developed Monte Carlo code. The calculated response is shown in Fig. 8 and given in Table 9.

2.3.6 Neutron rem counter

A neutron dose equivalent detector, neutron rem counter NSN10001 (Fuji Co. Ltd.), was used for measuring neutron dose equivalent rates on the beam axis behind the shield. The thermal neutron detector, 5.08-cm-diameter spherical proportional counter filled with 5 atm ^{3}He gas, are inserted at the center of a 21.0-cm-diameter spherical polyethylene moderator. The moderator is well arranged in terms of its material and geometry so that the response function of the rem counter reproduces the curve of the fluence-to-dose-equivalent conversion factor given by ICRP21[21] as close as possible. The sensitivity of the rem counter is 50 cps per mrem/h, which is calibrated with a ^{252}Cf neutron source.

3. RESULTS

3.1 Neutron spectra measured with the BC501A scintillation counter

The transmitted neutron energy spectra measured with a BC501A scintillation counter are shown in Figs. 9 - 14 and their data are tabulated in Table 10 - 15. The absolute fluxes are given as lethargy fluxes normalized to unit proton beam charge (μC). Figures 9, 10, 12 and 13 show the spectra on the beam axis and 20 and 40 cm off the beam axis behind 25- and 50-cm thick concrete shield, on the other hand, Figs. 11 and 14 show the spectra on the beam axis behind the concrete shields of up to 150 and 200 cm thickness for 43- and 68-MeV p-Li experiments, respectively. The experimental errors of the spectra in the figures include errors of spectrum unfolding and counting statistics in the measurement, conversion factor of fluence monitor counts to total charge of proton beam (3%), neutron penetration factor through objects on the beam line (3%) and the fluence monitor counting statistics (less than 1%).

3.2 Counting rates and neutron spectra measured with the Bonner ball counter

Counting rates behind the concrete shields up to 150 cm thickness on the beam axis were measured using the Bonner ball counter and are given in Table 16 and 17. Unfolded neutron spectra are shown in Figs. 15 and 16, and the numerical data are given in Tables 18 and 19 for 43- and 68-MeV p-^{7}Li neutron experiments, respectively. The experimental errors of the neutron spectra unfolded with the SAND-2 unfolding code are considered to be 50 to 200 %.

3.3 Fission rates and reaction rates measured with fission counters, TLDs and SSNTD

Fission rates were measured behind the shields of various thickness using ^{238}U and ^{232}Th fission counters. The positions were along the beam axis and 20 cm from the beam axis. The results are shown in Figs.17 and 18, and given in Tables 20 and 21 for 43- and 68-MeV p-^{7}Li neutron experiments, respectively. The fission rates correspond to the integrated neutron flux in the energy region above ~1 MeV where their fission cross sections are dominant.

The differences of reaction rates between ^{7}LiF and ^{nat}LiF TLDs placed inside 150- and 200-cm thick concrete shields are shown in Fig.19 and are given in Table 22. The differences are dominated by the neutrons in the energy region lower than 1 MeV as shown in Fig. 7.

The reaction rates of SSNTD measured inside the concrete shield are shown in Fig. 20 and given in Table 23. As shown in Fig.8, the efficiency of the detector is dominated by the neutrons in the energy region lower than about 10 MeV.

The errors of these three kinds of measured data include the statistical error of each detector counting and other errors described in section 3.1.

3.4 Neutron dose equivalent

The neutron dose equivalent data measured with a neutron rem counter are tabulated in Table 24. Neutron dose equivalents were also estimated from the measured neutron spectra and the ICRP21 neutron-flux-to-dose-equivalent conversion factor[21], and are given in Table 25. The measured neutron spectra were obtained from the results above 10 MeV of the BC501A scintillation counter and those below 10 MeV of the Bonner ball counter. The dose equivalents at 0 cm thickness are estimated using source neutron spectra tabulated in Tables 3 and 4, and peak fluxes, 1.96×10^4 and 2.49×10^4 [n cm^{-2} μC^{-1}] at the rotary shutter exit for 43- and 68-MeV p-^{7}Li neutron experiments, respectively. No additional iron collimator was used in front of the shield assembly in the neutron rem counter measurement, the neutron spectra behind 25- and 50-cm thick concrete were, however, measured on the geometry having the additional iron collimator. The estimated dose equivalents were, therefore, corrected to those without the additional collimator. The correction factors are the ratio of injecting neutron fluxes at the surface of shield without / with the additional collimators, which are 1.96/1.77 and 2.49/2.06 for 43- and 68-MeV p-^{7}Li neutron experiments, respectively. The neutron dose equivalents are compared in Fig.21.

ACKNOWLEDGMENT

We wish to thank the operation staff of the TIARA facility for their helpful cooperation during the experiment. This work was conducted as a Universities-JAERI Collaborative Project Research Program.

The errors of these three kinds of measured data include the statistical error of each detector counting and other errors described in section 3.1.

3.4 Neutron dose equivalent

The neutron dose equivalent data measured with a neutron rem counter are tabulated in Table 24. Neutron dose equivalents were also estimated from the measured neutron spectra and the ICRP21 neutron-flux-to-dose-equivalent conversion factor[21], and are given in Table 25. The measured neutron spectra were obtained from the results above 10 MeV of the BC501A scintillation counter and those below 10 MeV of the Bonner ball counter. The dose equivalents at 0 cm thickness are estimated using source neutron spectra tabulated in Tables 3 and 4, and peak fluxes, 1.96×10^4 and 2.49×10^4 [n cm^{-2} μC^{-1}] at the rotary shutter exit for 43- and 68-MeV p-^{7}Li neutron experiments, respectively. No additional iron collimator was used in front of the shield assembly in the neutron rem counter measurement, the neutron spectra behind 25- and 50-cm thick concrete were, however, measured on the geometry having the additional iron collimator. The estimated dose equivalents were, therefore, corrected to those without the additional collimator. The correction factors are the ratio of injecting neutron fluxes at the surface of shield without / with the additional collimators, which are 1.96/1.77 and 2.49/2.06 for 43- and 68-MeV p-^{7}Li neutron experiments, respectively. The neutron dose equivalents are compared in Fig.21.

ACKNOWLEDGMENT

We wish to thank the operation staff of the TIARA facility for their helpful cooperation during the experiment. This work was conducted as a Universities-JAERI Collaborative Project Research Program.

REFERENCES

1. Meulders J. P., Leleux P., Macq P. C., Pirart C. and Valenduc G., " Intensity Measurements and Shielding of a Fast-neutron Beam for Biological and Medical Applications," Nucl. Instrum. Methods., 126, 81 (1975).
2. Shin K., Ishii Y., Uwamino Y., Sakai H. and Numata S., "Transmission of medium energy neutrons through concrete shields," Radi. Pro. Dosi., 37, No.3, 175 (1991).
3. Uwamino Y., Nakamura T. and Shin K., " Penetration Through Shielding Materials of Secondary Neutrons and Photons Generated by 52-MeV Protons," Nucl. Sci. Eng., 80, 360 (1982).
4. Ishikawa T., Miyama Y. and Nakamura T., "Neutron Penetration Through Iron and Concrete Shields with the Use of 22.0- and 32.5-MeV Quasi-Monoenergetic Sources," Nucl. Sci. Eng., 116, 278 (1994).
5. Moritz L. E., "Measurement of Neutron Leakage Spectra at a 500-MeV Proton Accelerator," Health Phys, 56, No.3, 278 (1989).
6. Nakao N., Nakashima H., Nakamura T., Tanaka Sh., Tanaka Su., Shin K., Baba M., Sakamoto Y. and Nakane Y., "Transmission through shields of quasi-monoenergetic neutrons generated by 43- and 68-MeV Protons : Part I - Concrete Shielding Experiment and Calculation for Practical Application," Nucl. Sci. Eng., 124,228 (1996).
7. Nakashima H., Nakao N., Tanaka Sh., Nakamura T., Shin K., Tanaka Su., Takada H., Meigo S., Sakamoto Y., Nakane Y. and Baba M., "Transmission through shields of quasi-monoenergetic neutrons generated by 43- and 68-MeV Protons : Part II - Iron Shielding Experiment and Analysis for Investigating Calculation Methods and Cross Section Data," Nucl. Sci. Eng., 124,243 (1996).
8. Nakashima H., Nakao N., Tanaka Sh., Nakamura T., Shin K., Tanaka Su., Meigo S., Nakane Y., Takada H., Sakamoto Y. and Baba M., "Experiments on Iron Shield Transmission of Quasi-monoenergetic Neutrons Generated by 43- and 68-MeV Protons via the ^{7}Li(p,n) reaction", JAERI-Data/Code 96-005 (1996).
9. Baba M., Iwasaki T., Kiyosumi T., Yoshioka Y., Matsuyama S., Hirakawa N., Nakamura T., Tanaka Su., Tanaka Sh., Nakashima H., Meigo S. and Tanaka R., "Characterization and Application of 20-90 MeV ^{7}Li(p,n) Neutron Source at TIARA," Proceedings of International Conference on Nuclear Data for Science and Technology, Gatlinburg Tennessee, U.S.A., Vol.1, 90, (1994).
10. Shin K., Uwamino Y. and Hyodo T., "Propagation of errors from response functions to unfolded spectrum," Nucl. Technol., 53,78 (1981).

11. Nakao N., Nakamura T., Baba B., Uwamino Y., Nakanishi N., Nakashima H. and Tanaka Sh., "Measurements of response function of organic liquid scintillator for neutron energy range up to 135MeV," Nucl. Instrum. Methods., A362, 454 (1995).
12. McElroy W. N., Berg S., Crockett T. and Hawkins R. G., "A computer automated iterative method for neutron flux spectra determination by foil activation," AFWL-TR-67-41, Air Force Weapons Laboratory, Kirtland Air Force Base, vol. 1-4 (1967).
13. Uwamino Y., Nakamura T. and Hara A., "Two types of multi-moderator neutron spectrometers : gamma-ray insensitive type and high-efficiency type," Nucl. Instrum. Methods., A239, 299 (1985).
14. Straker G. R., Steven P. N., Irving D. C. and Cain V. R., "MORSE Code - A Multigroup Neutron and Gamma Ray Monte Carlo Transport Code," ORNL-4585, Oak Ridge National Laboratory, (1970).
15. Alsmiller Jr. R. G., Barnes J. M. and Drischler J. D., "Neutron-Photon Multigroup Cross Sections for Neutron Energies up to 400 MeV (Revision 1)," ORNL/TM-9801, Oak Ridge National Laboratory (1986).
16. Yoshizawa M., Private communication.
17. Shibata K. et al., "Japanese Evaluated Nuclear Data Library, Version-3 -JENDL-3-," JAERI 1319, Japan Atomic Energy Research Institute (1990).
18. Lisowski P. W. et al., "Neutron Induced Fission Cross Section Rates for ^{232}Th, ^{235,238}U, ^{237}Np and ^{239}Pu from 1 to 400 MeV," Proc. Int. Conf. Nuclear Data for Sci. and Technol., Mito, Japan, p.97-99 (1988).
19. Lisowski P. W. et al., "Fission Cross Sections in the Intermediate Energy Region," Proc. Spec. Meet. on Neutron Cross Section Standards for the Energy Region above 20 MeV, Uppsala, Sweden, 21-23 May, 1991, p.177-186 (1991).
20. Hashikura H., Haikawa K., Tanaka S. and Kondo K., "Calculation of Neutron Response of Thermoluminescent Dosimeters," J. Faculty of Eng., Univ. of Tokyo, 39(1), 7 (1987).
21. "Data for Use in Protection Against External Radiation," Ann. ICRP, 17, 2/3 (1987).

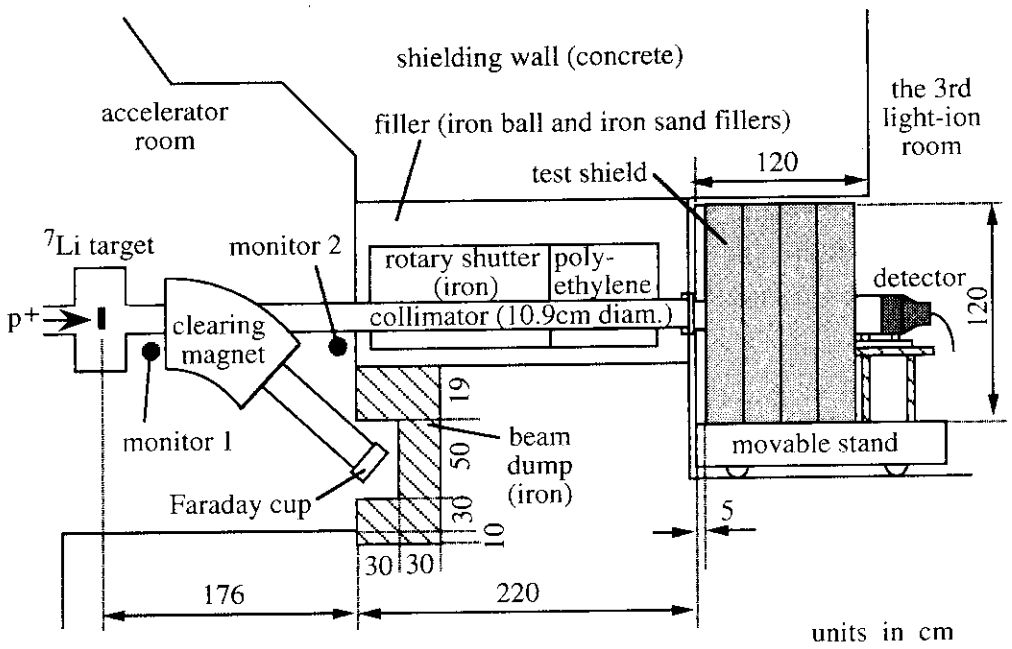

Fig.1 Cross sectional view of the TIARA neutron facility with the experimental arrangement.

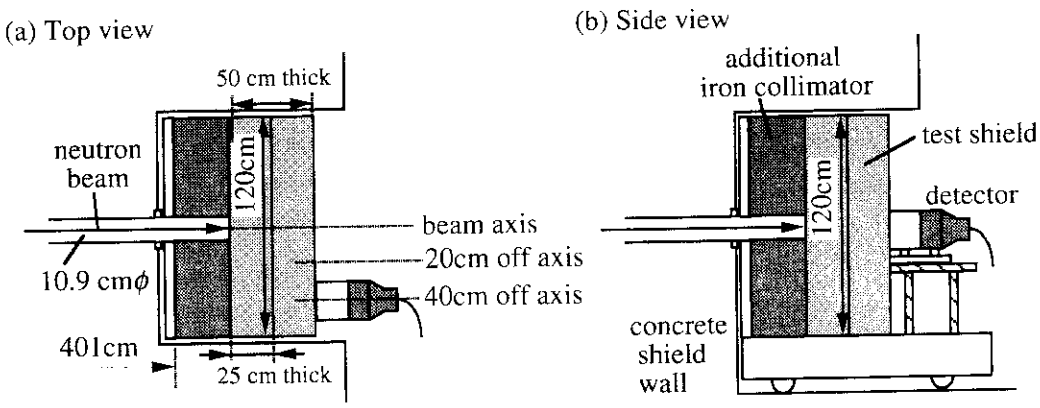

Fig.2 Experimental arrangement for 25- and 50-cm thick concrete shield with additional iron collimator.

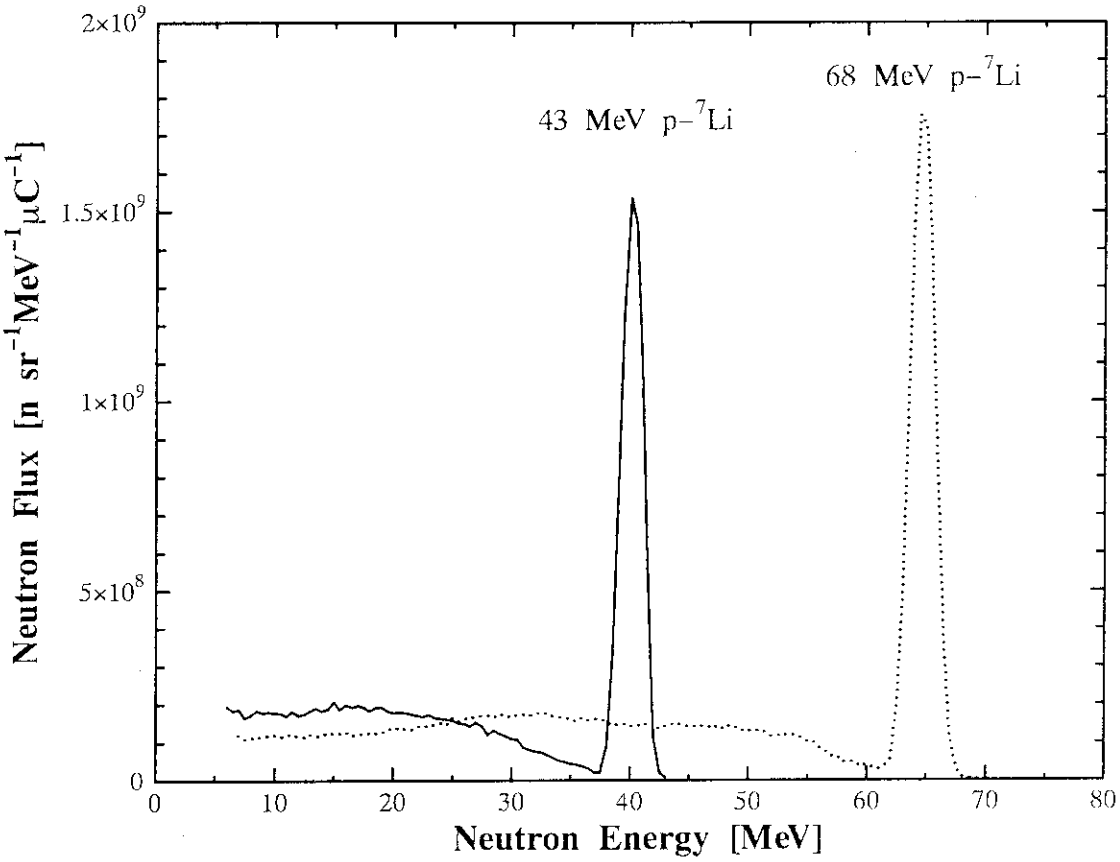

Fig.3 Energy spectra of source neutrons generated by ^{7}Li(p,n) reaction using 43- and 68-MeV protons. These spectra were obtained by TOF measurements and the absolute peak fluxes were given by PRT measurements. The low energy limit of the spectra obtained by the TOF measuremnts are 7 MeV.

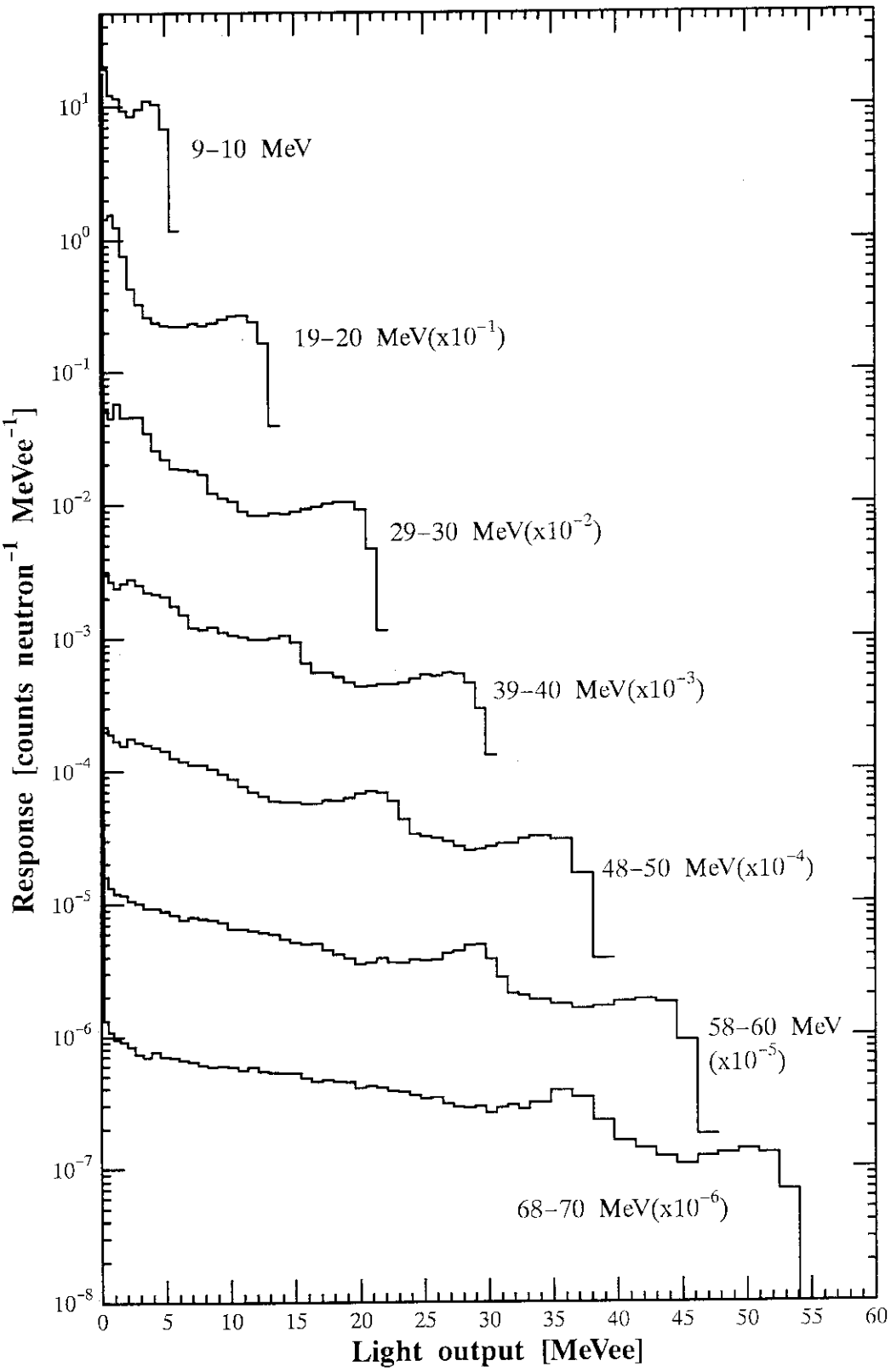

Fig.4 Responses of BC501A scintillation counter to neutrons.

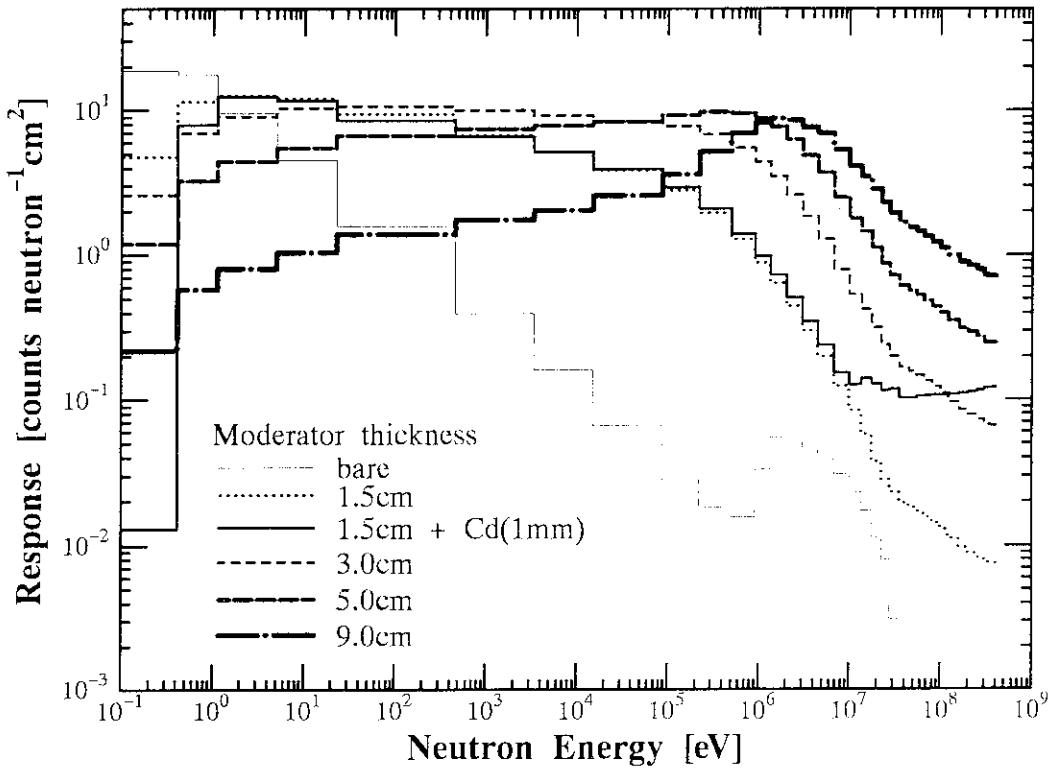

Fig.5 Responses of the Bonner ball counter to neutrons for each moderator thickness.

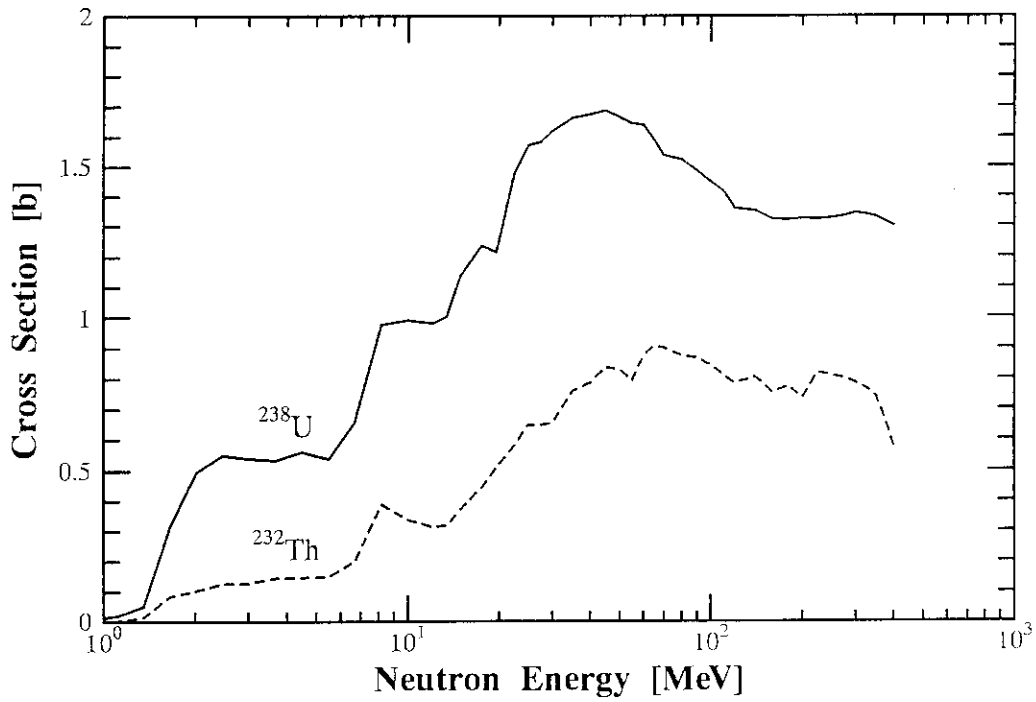

Fig.6 Fission cross sections of ^{238}U and ^{232}Th. The cross sections up to 20 MeV is taken from JENDL−3, and those between 20 to 400 MeV are quoted from the data measured by Lisowski et al.

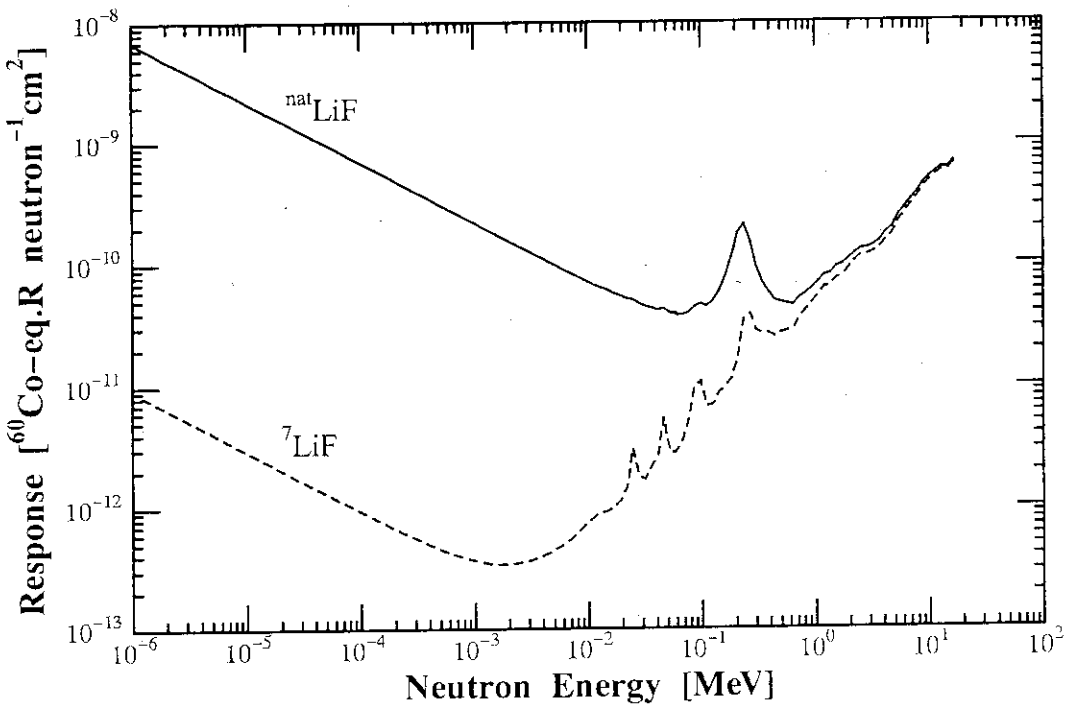

Fig.7 Responses of ^{7}LiF and ^{nat}LiF TLDs to neutrons calculated using a code developed by Hashikura et al.

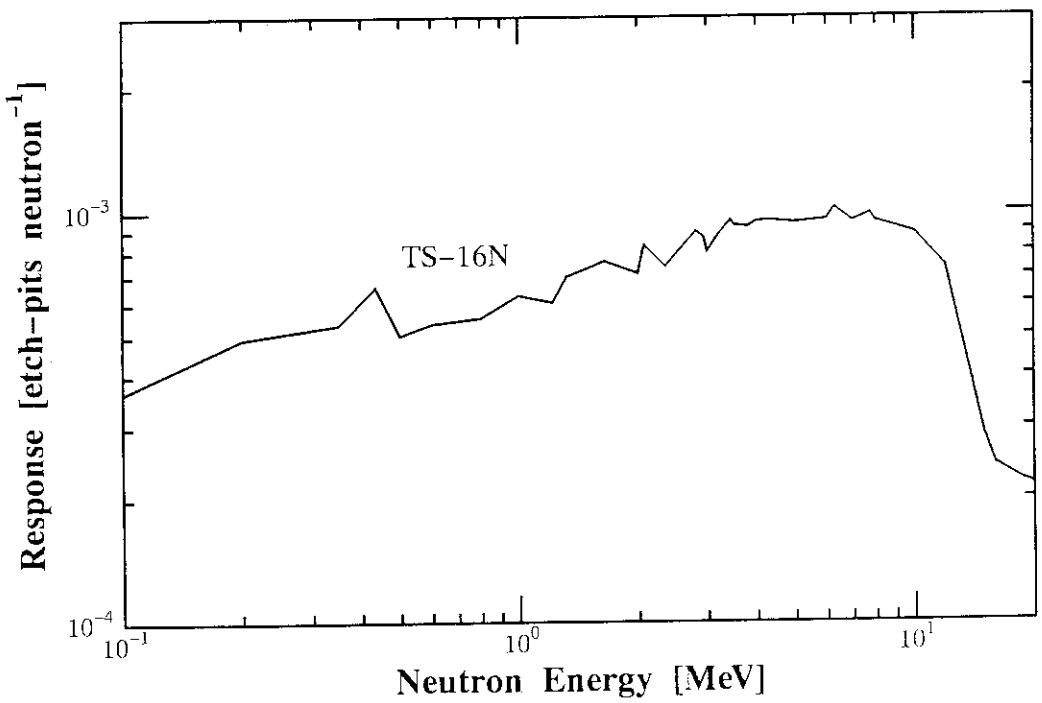

Fig.8 Calculated response of SSNTD to neutrons.

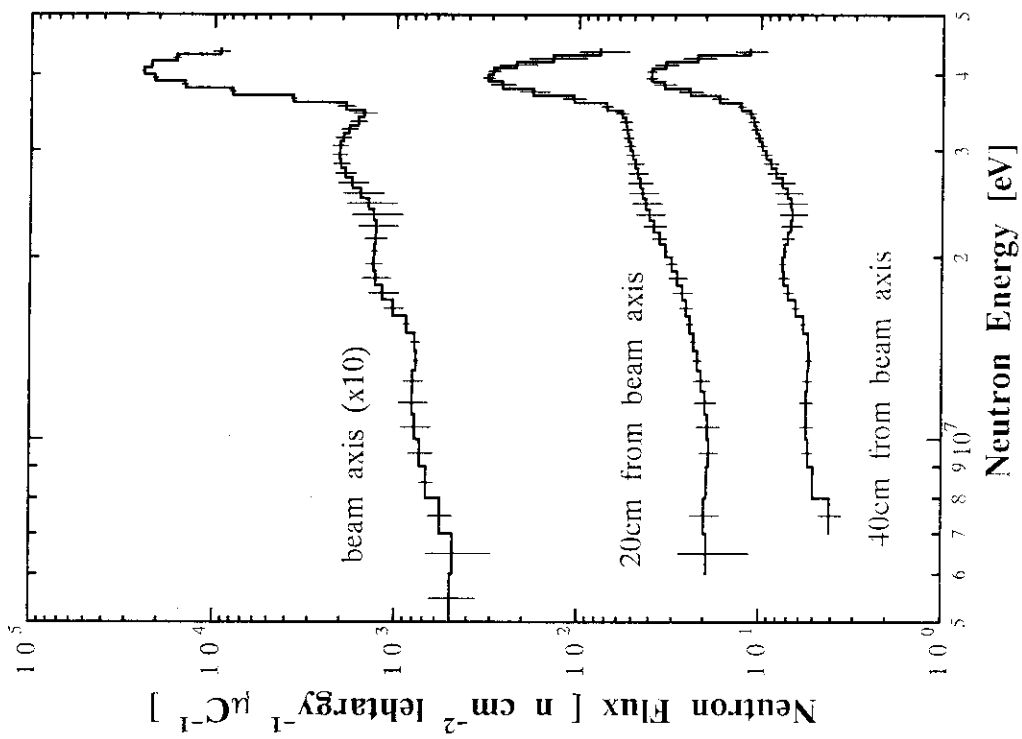

Fig.10 Neutron spectra behind 50-cm thick concrete shield measured with BC501A detector for 43 MeV p-^{7}Li neutrons.

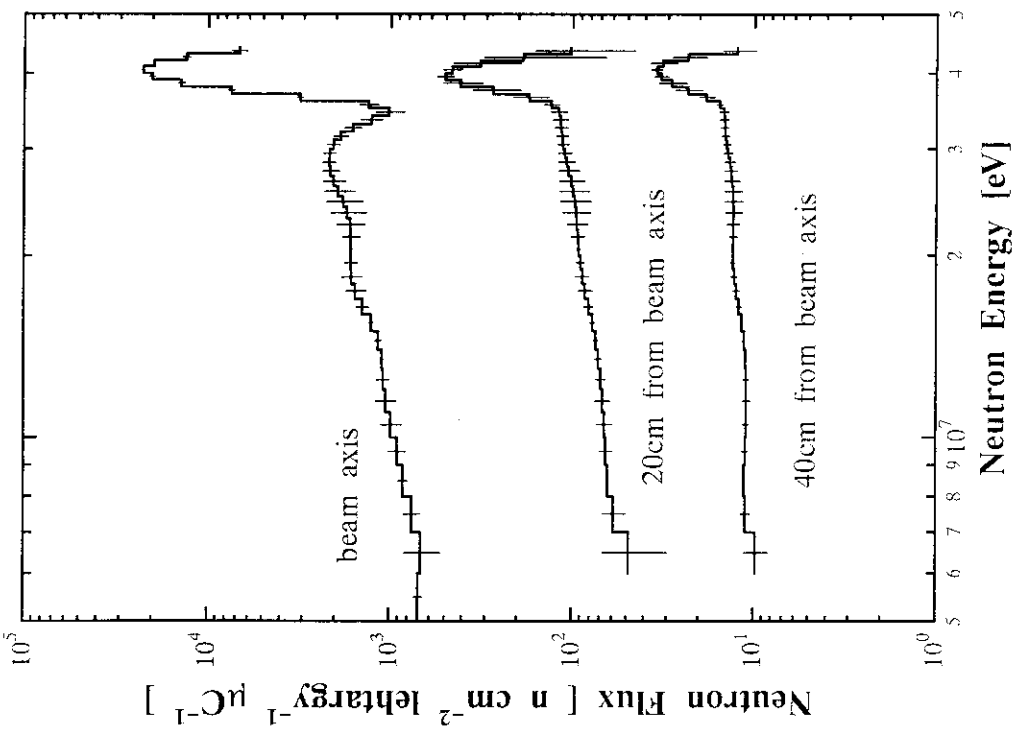

Fig.9 Neutron spectra behind 25-cm thick concrete shield measured with BC501A detector for 43 MeV p-^{7}Li neutrons.

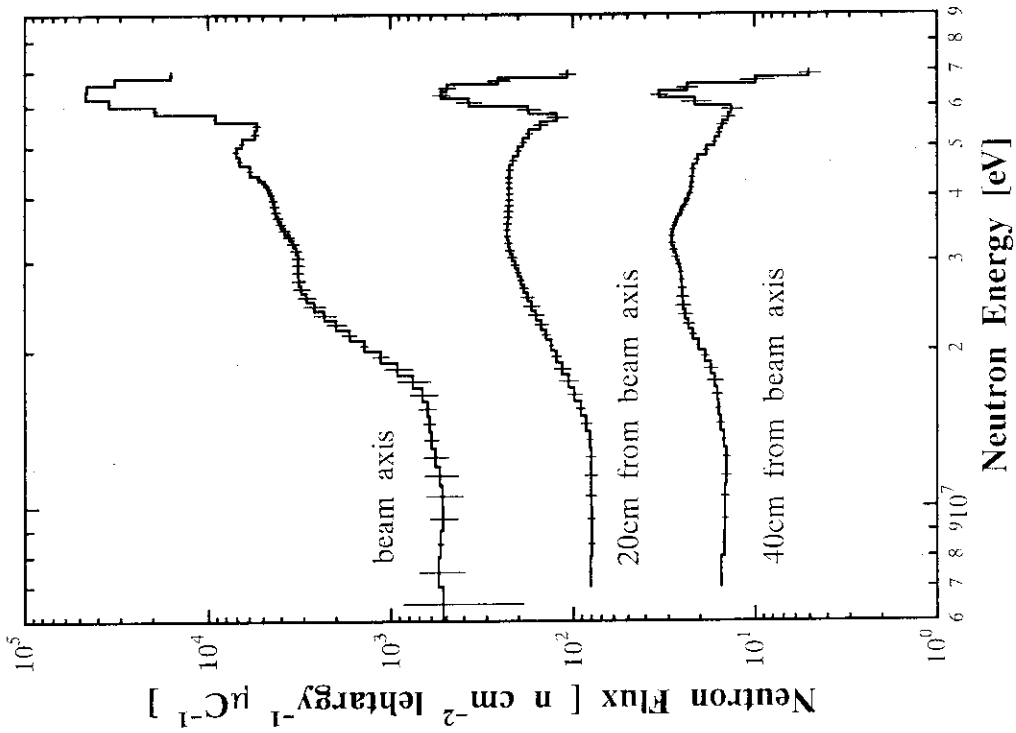

Fig.12 Neutron spectra behind 25-cm thick concrete shield measured with BC501A detector for 68 MeV p-^{7}Li neutrons.

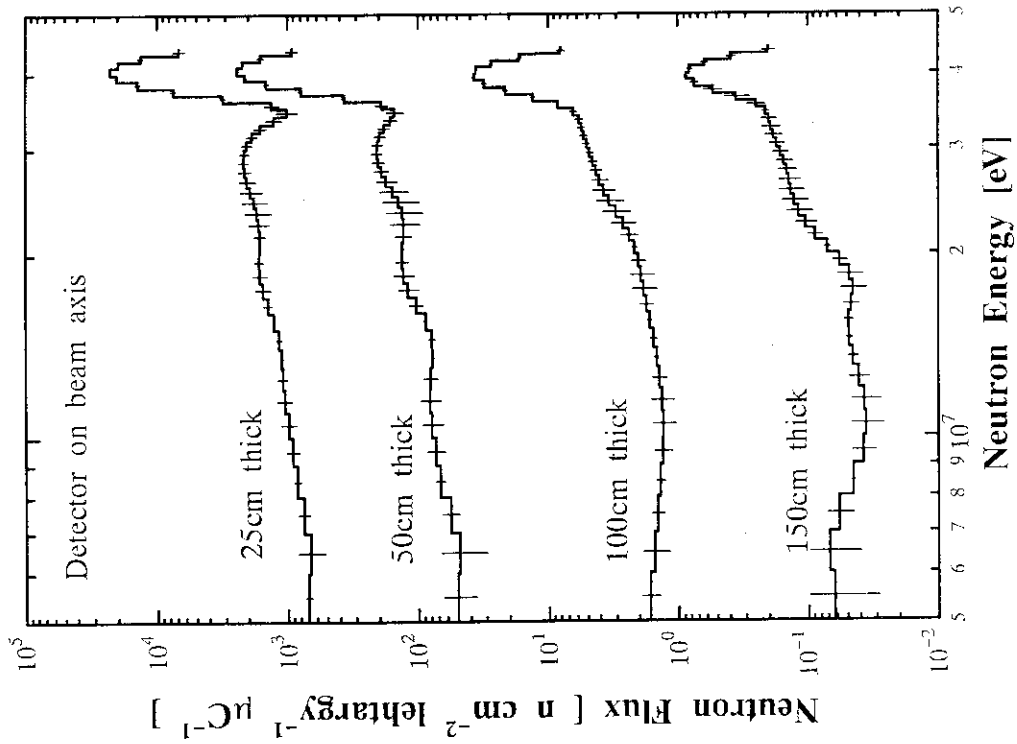

Fig.11 Neutron spectra behind various thickness concrete shields measured with BC501A detector on the beam axis for 43 MeV p-^{7}Li neutrons.

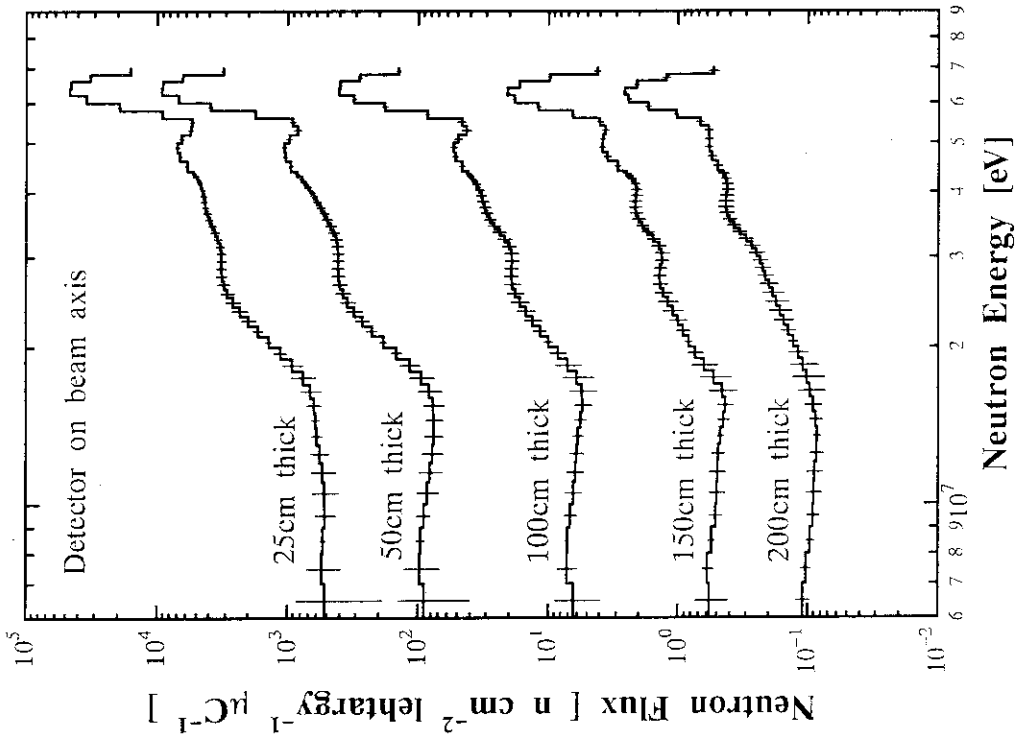

Fig.14 Neutron spectra behind various thickness concrete shields measured with BC501A detector on the beam axis for 68 MeV p−^{7}Li neutrons.

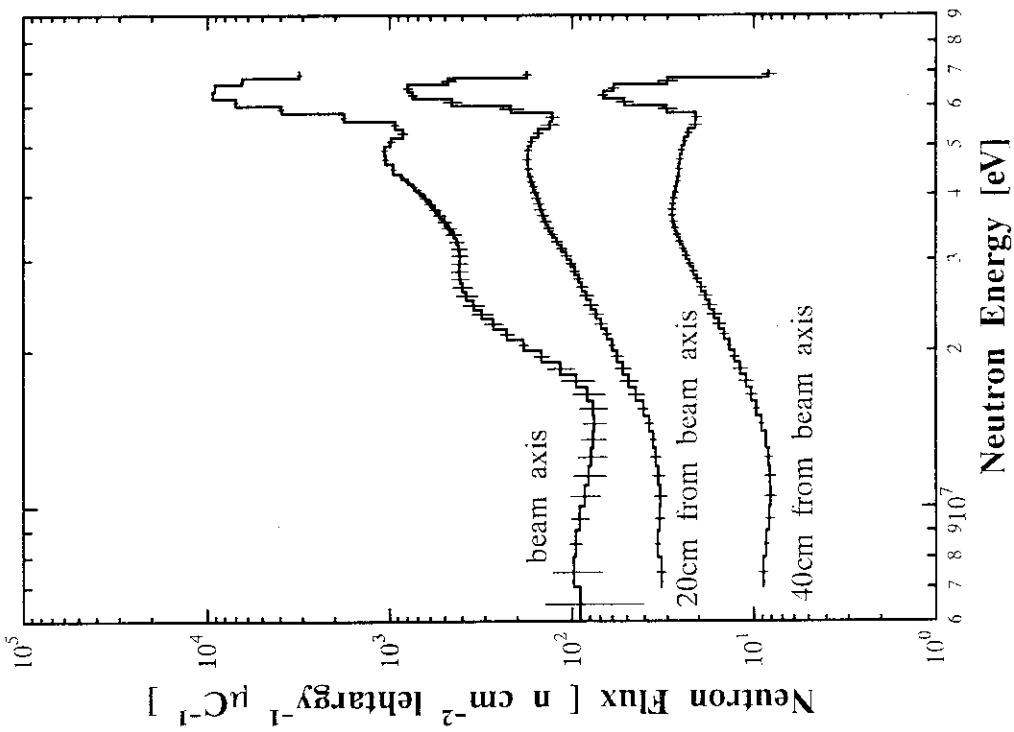

Fig.13 Neutron spectra behind 50−cm thick concrete shield measured with BC501A detector for 68 MeV p−^{7}Li neutrons.

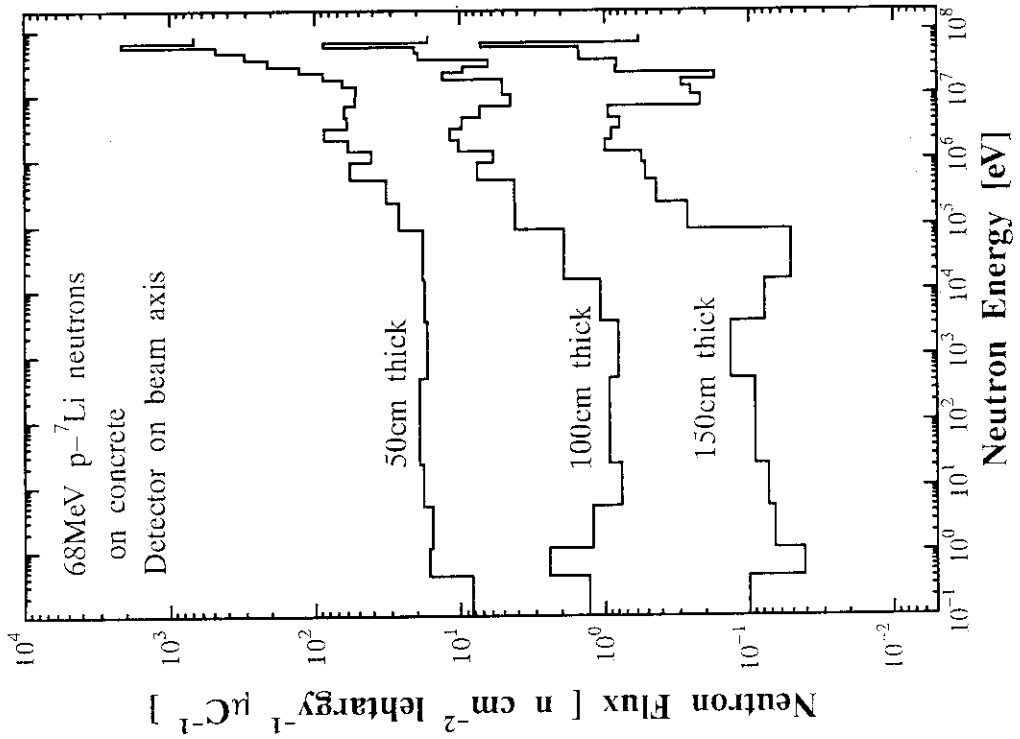

Fig.16 Neutron spectra behind various thickness concrete shields measured with Bonner ball detector for 68 MeV p−^{7}Li neutrons.

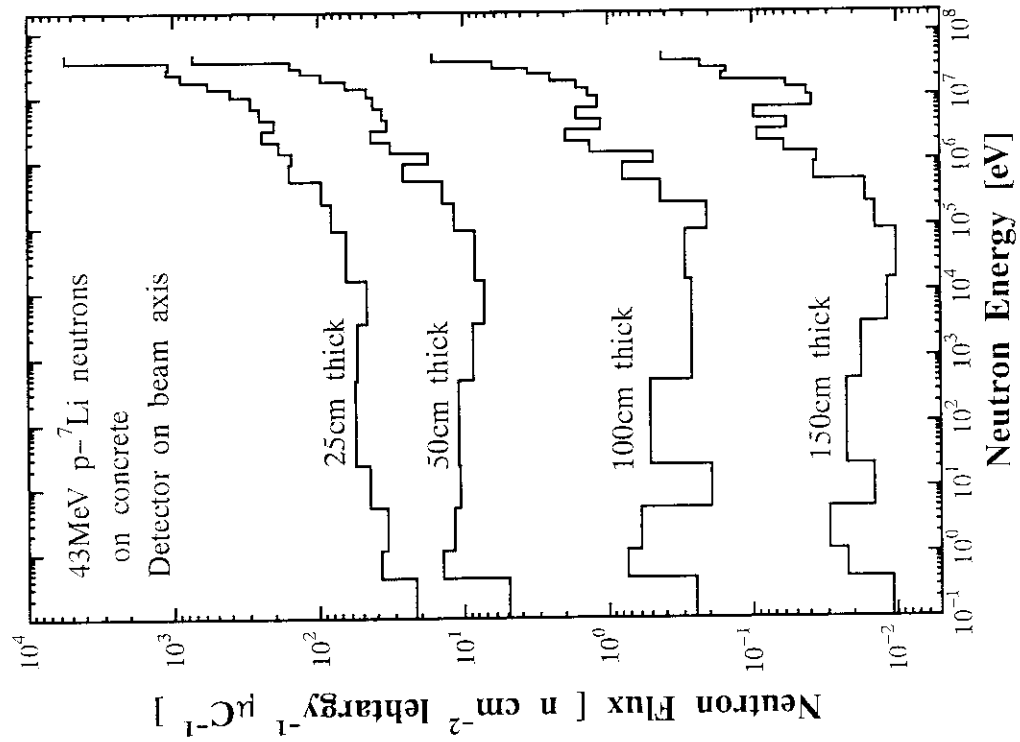

Fig.15 Neutron spectra behind various thickness concrete shields measured with Bonner ball detector for 43 MeV p−^{7}Li neutrons.

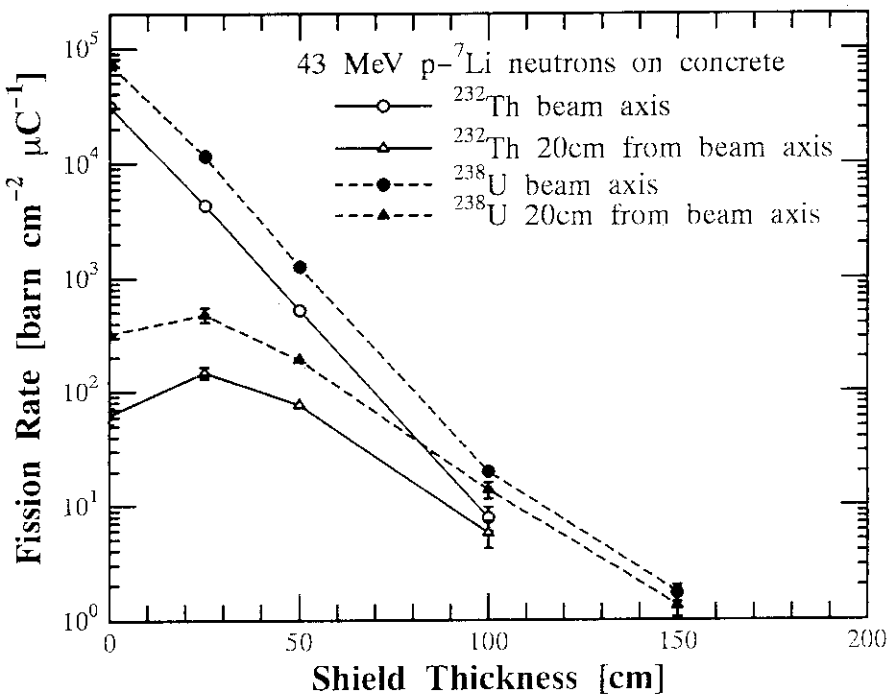

Fig.17 Measured fission rates of ^{238}U and ^{232}Th behind concrete shield for 43 MeV p−^{7}Li neutrons.

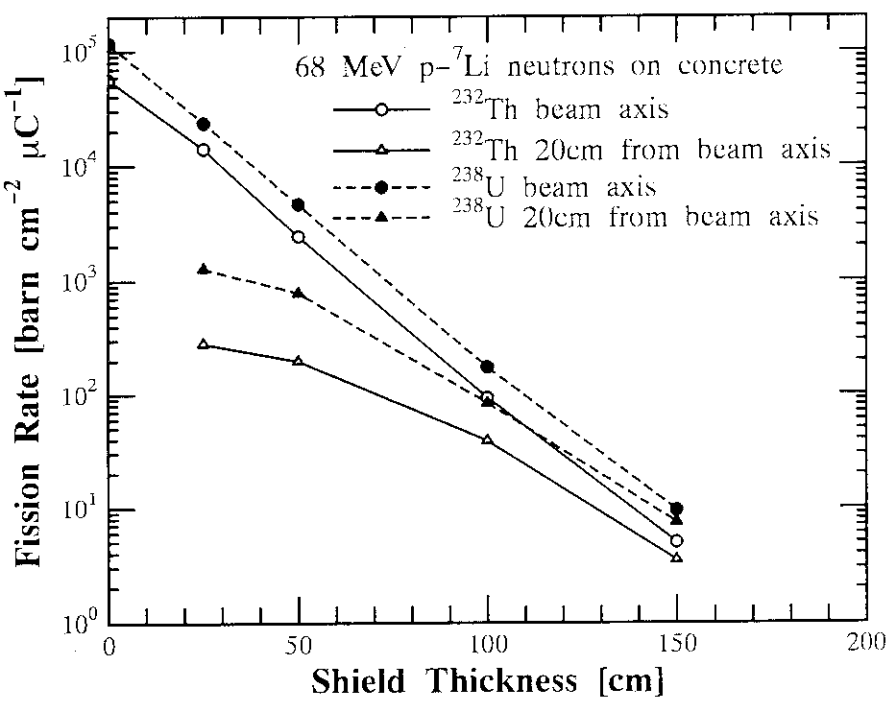

Fig.18 Measured fission rates of ^{238}U and ^{232}Th behind concrete shield for 68 MeV p−^{7}Li neutrons.

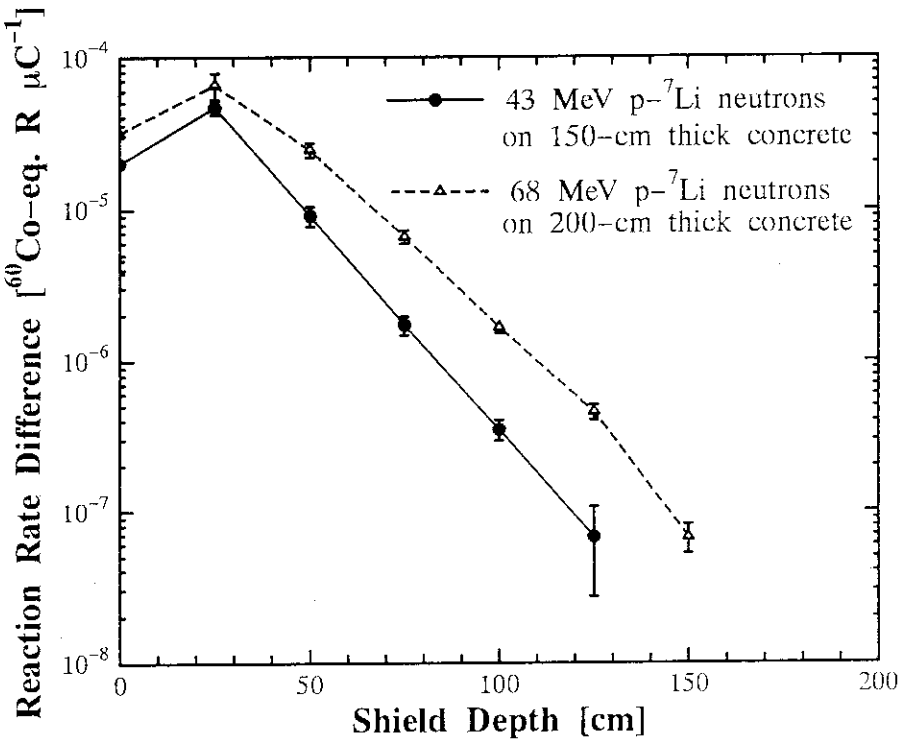

Fig.19 Defference between reaction rates of ^{7}LiF and ^{nat}LiF TLDs inside concrete shields for 43- and 68-MeV p-^{7}Li neutrons. Detectors were placed on the beam axis.

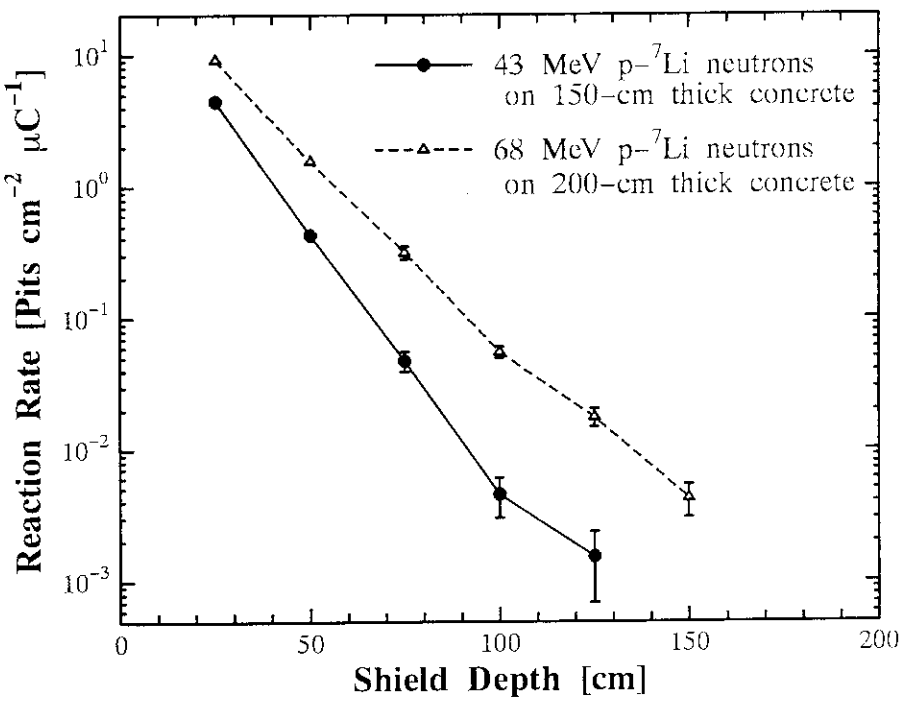

Fig.20 Measured reaction rates of SSNTD inside concrete shields for for 43- and 68-MeV p-^{7}Li neutrons. Detectors were placed on the beam axis.

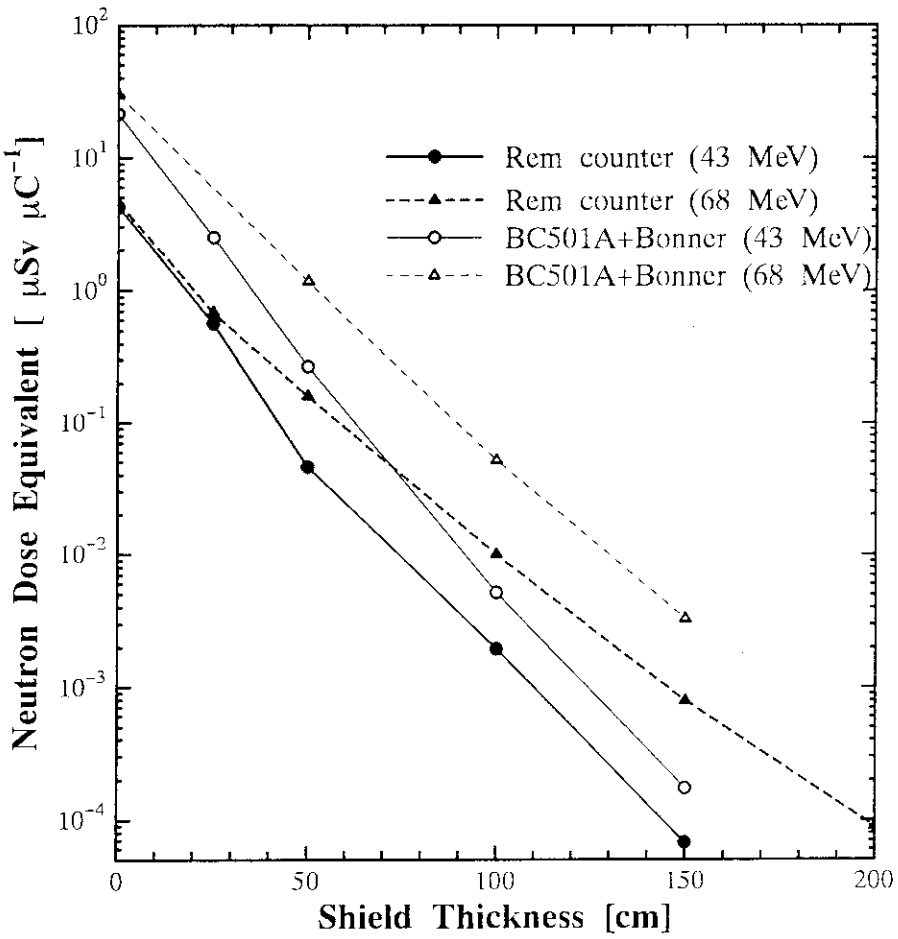

Fig.21 Neutron dose equivalent measured with the rem counter for 43- and 68-MeV p-^{7}Li neutrons. Neutron dose equivalent estimated from neutron spectra measured with BC501A and Bonner ball detectors are also shown.

Table 1 Density and atomic compositions of the concrete shield and the iron collimator.

Material	Density [g cm^{-3}]	Atom	Atomic Density [x10^{22} cm^{-3}]
Concrete	2.31	Hydrogen	1.498
		Oxygen	4.188
		Sodium	0.123
		Magnesium	0.062
		Aluminum	0.312
		Silicon	1.110
		Potassium	0.038
		Calcium	0.430
		Iron	0.141
Iron	7.87	Iron	8.487

Table 2 Dimensions of the concrete shield and additional collimator, and detector positions.

Ep [a] [MeV]	Shield Thickness [cm]	Collimator Thickness [cm]	Peak Flux of Source Neutron [x10^{9} n/sr/μC]	Detector Position (distance from beam axis) [cm]					
				BC501A	Bonner [b]	F.C.[c]	TLD [d]	SSNTD [e]	Rem[f]
43	25	0	3.15	-	-	0, 20	0	0	0
	25	40	3.45	0, 20, 40	0	-	-	-	-
	50	0	3.15	-	-	0, 20	0	0	0
	50	40	3.45	0, 20, 40	0	-	-	-	-
	100	0	3.15	0	0	0, 20	0	0	0
	150	0	3.15	0	0	-	-	-	-
68	25	0	4.00	-	-	0, 20	0	0	0
	25	80	4.77	0, 20, 40	-	-	-	-	-
	50	0	4.00	-	-	0, 20	0	0	0
	50	80	4.77	0, 20, 40	0	-	-	-	-
	100	0	4.00	0	0	0, 20	0	0	0
	150	0	4.00	0	0	0, 20	0	0	0
	200	0	4.00	0	-	-	-	-	-

TLD and SSNTD detectors were placed inside the concrete shields. The other detectors were placed behind the concrete shields of each thickness.

a Proton energy

b Bonner ball counter

c ^{238}U and ^{232}Th fission counters

d ^{7}LiF and ^{nat}LiF TLDs

e Solid state nuclear track detector

f Rem counter

Table 3 Energy spectrum of 43-MeV p-^{7}Li source neutrons.

Energy Boundary [MeV]	Flux	Error	Energy Boundary [MeV]	Flux	Error
- 6.5[a]	4.405E-02[b]		25.5 - 26.5	4.097E-02	1.77E-03
			26.5 - 27.5	3.960E-02	1.70E-03
6.5 - 7.5	4.405E-02	1.51E-03	27.5 - 28.5	3.473E-02	1.50E-03
7.5 - 8.5	4.423E-02	1.52E-03	28.5 - 29.5	3.491E-02	1.51E-03
8.5 - 9.5	4.483E-02	1.54E-03	29.5 - 30.5	3.081E-02	1.34E-03
9.5 - 10.5	4.503E-02	1.54E-03	30.5 - 31.5	2.639E-02	1.16E-03
10.5 - 11.5	4.390E-02	1.51E-03	31.5 - 32.5	2.097E-02	9.43E-04
11.5 - 12.5	4.501E-02	1.51E-03	32.5 - 33.5	1.875E-02	1.19E-03
12.5 - 13.5	4.633E-02	1.57E-03	33.5 - 34.5	1.490E-02	9.60E-04
13.5 - 14.5	4.931E-02	1.65E-03	34.5 - 35.5	1.290E-02	8.40E-04
14.5 - 15.5	4.895E-02	1.65E-03	35.5 - 36.5	1.083E-02	7.11E-04
15.5 - 16.5	4.885E-02	1.62E-03	36.5 - 37.5	7.232E-03	4.91E-04
16.5 - 17.5	4.752E-02	1.57E-03	37.5 - 38.5	1.337E-02	8.53E-04
17.5 - 18.5	4.977E-02	1.63E-03	38.5 - 39.5	1.377E-01	8.31E-03
18.5 - 19.5	4.611E-02	1.51E-03	39.5 - 40.5	3.629E-01	2.18E-02
19.5 - 20.5	4.707E-02	1.56E-03	40.5 - 41.5	3.677E-01	2.21E-02
20.5 - 21.5	4.749E-02	2.05E-03	41.5 - 42.5	1.135E-01	6.86E-03
21.5 - 22.5	4.686E-02	2.02E-03	42.5 - 43.5	5.063E-03	3.54E-04
22.5 - 23.5	4.653E-02	2.01E-03	43.5 - 44.5	6.359E-04	7.29E-05
23.5 - 24.5	4.488E-02	1.91E-03	44.5 - 45.5	1.634E-04	3.31E-05
24.5 - 25.5	4.358E-02	1.88E-03			

The flux at monoenergetic peak (36.3-45.5 MeV) is normalized to unity.
The absolute peak flux for each experiment can be obtained from Table 2.
Ratio of the peak flux to the total flux above 6.5 MeV is 1:2.17.
a Neutron flux per unit energy blow 6.5 MeV is assumed to be constant, the value between 6.5-7.5 MeV.
b Read as 4.405 x 10^{-2}.

Table 4 Energy spectrum of 68-MeV p-^{7}Li source neutrons.

Energy Boundary [MeV]	Flux	Error	Energy Boundary [MeV]	Flux	Error
- 6.5[a]	2.373E-02[b]		38.5 - 39.5	3.399E-02	2.10E-03
			39.5 - 40.5	3.345E-02	2.07E-03
6.5 - 7.5	2.373E-02	8.50E-04	40.5 - 41.5	3.324E-02	2.05E-03
7.5 - 8.5	2.395E-02	8.55E-04	41.5 - 42.5	3.340E-02	2.07E-03
8.5 - 9.5	2.440E-02	8.67E-04	42.5 - 43.5	3.137E-02	1.94E-03
9.5 - 10.5	2.508E-02	8.86E-04	43.5 - 44.5	3.211E-02	1.98E-03
10.5 - 11.5	2.569E-02	9.07E-04	44.5 - 45.5	3.103E-02	1.92E-03
11.5 - 12.5	2.533E-02	8.98E-04	45.5 - 46.5	3.102E-02	1.92E-03
12.5 - 13.5	2.592E-02	9.21E-04	46.5 - 47.5	3.160E-02	1.95E-03
13.5 - 14.5	2.678E-02	9.46E-04	47.5 - 48.5	3.086E-02	1.90E-03
14.5 - 15.5	2.714E-02	9.60E-04	48.5 - 49.5	3.003E-02	1.85E-03
15.5 - 16.5	2.788E-02	9.83E-04	49.5 - 50.5	2.856E-02	1.77E-03
16.5 - 17.5	2.795E-02	9.89E-04	50.5 - 51.5	2.804E-02	1.73E-03
17.5 - 18.5	2.855E-02	1.01E-03	51.5 - 52.5	2.656E-02	1.64E-03
18.5 - 19.5	2.954E-02	1.04E-03	52.5 - 53.5	2.505E-02	1.56E-03
19.5 - 20.5	3.100E-02	1.09E-03	53.5 - 54.5	2.391E-02	1.48E-03
20.5 - 21.5	3.149E-02	1.10E-03	54.5 - 55.5	2.177E-02	1.36E-03
21.5 - 22.5	3.334E-02	1.45E-03	55.5 - 56.5	1.959E-02	1.22E-03
22.5 - 23.5	3.383E-02	1.46E-03	56.5 - 57.5	1.604E-02	1.01E-03
23.5 - 24.5	3.528E-02	1.52E-03	57.5 - 58.5	1.281E-02	8.38E-04
24.5 - 25.5	3.624E-02	1.56E-03	58.5 - 59.5	1.088E-02	7.42E-04
25.5 - 26.5	3.669E-02	1.57E-03	59.5 - 60.5	9.010E-03	6.27E-04
26.5 - 27.5	3.841E-02	1.64E-03	60.5 - 61.5	7.428E-03	5.27E-04
27.5 - 28.5	3.806E-02	1.62E-03	61.5 - 62.5	8.095E-03	5.62E-04
28.5 - 29.5	3.927E-02	1.67E-03	62.5 - 63.5	4.701E-02	2.90E-03
29.5 - 30.5	3.845E-02	1.64E-03	63.5 - 64.5	2.104E-01	1.27E-02
30.5 - 31.5	3.875E-02	1.65E-03	64.5 - 65.5	3.614E-01	2.18E-02
31.5 - 32.5	3.857E-02	1.64E-03	65.5 - 66.5	2.765E-01	1.67E-02
32.5 - 33.5	3.878E-02	2.39E-03	66.5 - 67.5	8.202E-02	4.99E-03
33.5 - 34.5	3.762E-02	2.33E-03	67.5 - 68.5	8.896E-03	6.05E-04
34.5 - 35.5	3.702E-02	2.28E-03	68.5 - 69.5	1.074E-03	1.12E-04
35.5 - 36.5	3.716E-02	2.30E-03	69.5 - 70.5	4.013E-04	6.17E-05
36.5 - 37.5	3.656E-02	2.26E-03	70.5 - 71.5	4.973E-04	6.87E-05
37.5 - 38.5	3.615E-02	2.23E-03	71.5 - 72.5	1.324E-04	3.24E-05

The flux at monoenergetic peak (60.8-72.5 MeV) is normalized to unity.
The absolute peak flux for each experiment can be obtained from Table 2.
Ratio of the peak flux to the total flux above 6.5 MeV is 1:2.61.
a Neutron flux per unit energy blow 6.5 MeV is assumed to be constant, the value between 6.5-7.5 MeV.
b Read as 2.373×10^{-2}.

Table 5 Response functions of BC501A scintillation counter.

Group No.	Light output [MeVee]	Upper Energy Boundary of Neutron Group [MeV] 1.0	2.0	3.0	4.0	5.0	6.0	7.0	8.0	9.0
1	0.196[a]	9.54E-01[b]	5.98E-01	3.37E-01	3.33E-01	2.98E-01	2.56E-01	2.38E-01	2.86E-01	2.78E-01
2	0.543	6.05E-03	3.29E-01	3.59E-01	1.68E-01	1.01E-01	7.14E-02	6.61E-02	5.96E-02	4.87E-02
3	0.983	0.0	7.06E-03	1.88E-01	2.46E-01	1.43E-01	8.54E-02	5.96E-02	5.52E-02	4.89E-02
4	1.486	0.0	0.0	7.89E-03	1.22E-01	1.78E-01	1.15E-01	7.28E-02	5.40E-02	4.68E-02
5	2.037	0.0	0.0	0.0	8.57E-03	9.97E-02	1.34E-01	9.33E-02	6.14E-02	4.35E-02
6	2.629	0.0	0.0	0.0	0.0	1.16E-02	7.84E-02	1.03E-01	7.84E-02	5.17E-02
7	3.256	0.0	0.0	0.0	0.0	0.0	7.79E-03	6.43E-02	8.06E-02	6.50E-02
8	3.911	0.0	0.0	0.0	0.0	0.0	0.0	8.21E-03	5.08E-02	6.39E-02
9	4.590	0.0	0.0	0.0	0.0	0.0	0.0	0.0	6.36E-03	4.31E-02
10	5.287	0.0	0.0	0.0	0.0	0.0	0.0	0.0	0.0	6.87E-03
11	6.002	0.0	0.0	0.0	0.0	0.0	0.0	0.0	0.0	0.0
		Group No. 12 through 60 same as above								

a Upper group boundary of light output in MeV-electron-equivalent. Lower boundary is 0 MeVee.
b 9.54×10^{-1} [counts neutron^{-1}]

Table 5 (continued)

Group No.	Upper Light [MeVee]	Upper Energy Boundary of Neutron Group [MeV] 10.0	11.0	12.0	13.0	14.0	15.0	16.0	17.0	18.0
1	0.196	2.72E-01	2.63E-01	2.87E-01	2.78E-01	2.64E-01	2.54E-01	2.72E-01	2.70E-01	2.56E-01
2	0.543	5.20E-02	5.49E-02	5.84E-02	6.93E-02	7.60E-02	7.69E-02	7.40E-02	6.95E-02	5.80E-02
3	0.983	4.09E-02	3.35E-02	3.06E-02	3.21E-02	3.98E-02	4.37E-02	5.00E-02	5.62E-02	6.40E-02
4	1.486	4.24E-02	3.79E-02	3.13E-02	2.71E-02	2.56E-02	2.93E-02	2.89E-02	3.45E-02	3.83E-02
5	2.037	3.80E-02	3.58E-02	3.04E-02	2.56E-02	2.21E-02	2.05E-02	1.96E-02	2.02E-02	2.27E-02
6	2.629	3.69E-02	3.35E-02	2.99E-02	2.57E-02	2.21E-02	1.95E-02	1.77E-02	1.70E-02	1.62E-02
7	3.256	4.39E-02	3.41E-02	2.94E-02	2.56E-02	2.25E-02	1.99E-02	1.74E-02	1.62E-02	1.51E-02
8	3.911	5.30E-02	3.93E-02	3.04E-02	2.59E-02	2.26E-02	1.98E-02	1.72E-02	1.56E-02	1.42E-02
9	4.590	5.15E-02	4.72E-02	3.57E-02	2.74E-02	2.28E-02	2.01E-02	1.73E-02	1.56E-02	1.41E-02
10	5.287	3.52E-02	4.42E-02	4.03E-02	3.12E-02	2.40E-02	2.03E-02	1.79E-02	1.59E-02	1.43E-02
11	6.002	6.18E-03	3.13E-02	3.68E-02	3.52E-02	2.79E-02	2.21E-02	1.84E-02	1.62E-02	1.45E-02
12	6.732	0.0	6.02E-03	2.68E-02	3.19E-02	3.07E-02	2.54E-02	2.04E-02	1.71E-02	1.50E-02
13	7.476	0.0	0.0	5.48E-03	2.34E-02	2.75E-02	2.74E-02	2.32E-02	1.87E-02	1.57E-02
14	8.232	0.0	0.0	0.0	4.66E-03	1.97E-02	2.43E-02	2.38E-02	2.09E-02	1.70E-02
15	8.999	0.0	0.0	0.0	0.0	4.29E-03	1.73E-02	2.12E-02	2.13E-02	1.87E-02
16	9.776	0.0	0.0	0.0	0.0	0.0	3.78E-03	1.53E-02	1.90E-02	1.89E-02
17	10.562	0.0	0.0	0.0	0.0	0.0	0.0	3.39E-03	1.36E-02	1.71E-02
18	11.357	0.0	0.0	0.0	0.0	0.0	0.0	0.0	3.07E-03	1.22E-02
19	12.159	0.0	0.0	0.0	0.0	0.0	0.0	0.0	0.0	2.90E-03
20	12.968	0.0	0.0	0.0	0.0	0.0	0.0	0.0	0.0	0.0
		Group No. 21 through 60 same as above								

Table 5 (continued)

Group No.	Upper Light [MeVee]	Upper Energy Boundary of Neutron Group [MeV] 19.0	20.0	21.0	22.0	23.0	24.0	25.0	26.0	27.0
1	0.196	2.65E-01	2.72E-01	2.70E-01	2.63E-01	2.65E-01	2.65E-01	2.68E-01	2.69E-01	2.69E-01
2	0.543	4.06E-02	3.97E-02	3.24E-02	2.90E-02	2.46E-02	2.17E-02	2.02E-02	1.85E-02	1.76E-02
3	0.983	6.77E-02	5.43E-02	4.57E-02	3.43E-02	2.74E-02	2.44E-02	2.05E-02	1.81E-02	1.69E-02
4	1.486	4.75E-02	4.62E-02	5.31E-02	5.48E-02	4.75E-02	3.81E-02	3.16E-02	2.68E-02	2.47E-02
5	2.037	2.52E-02	3.07E-02	3.11E-02	3.58E-02	3.88E-02	3.96E-02	3.95E-02	3.26E-02	2.71E-02
6	2.629	1.73E-02	1.86E-02	2.32E-02	2.29E-02	2.31E-02	2.40E-02	2.74E-02	2.89E-02	2.93E-02
7	3.256	1.45E-02	1.48E-02	1.49E-02	1.71E-02	1.90E-02	1.96E-02	1.84E-02	1.85E-02	2.01E-02
8	3.911	1.33E-02	1.24E-02	1.25E-02	1.22E-02	1.40E-02	1.56E-02	1.53E-02	1.54E-02	1.45E-02
9	4.590	1.30E-02	1.17E-02	1.07E-02	1.10E-02	1.11E-02	1.25E-02	1.26E-02	1.19E-02	1.28E-02
10	5.287	1.29E-02	1.14E-02	1.03E-02	9.98E-03	1.02E-02	1.01E-02	1.04E-02	1.13E-02	1.08E-02
11	6.002	1.28E-02	1.15E-02	1.01E-02	9.54E-03	8.87E-03	9.29E-03	8.85E-03	9.19E-03	1.05E-02
12	6.732	1.38E-02	1.17E-02	1.05E-02	9.46E-03	8.71E-03	8.31E-03	8.80E-03	8.65E-03	8.66E-03
13	7.476	1.40E-02	1.25E-02	1.06E-02	9.50E-03	8.80E-03	8.07E-03	7.66E-03	8.23E-03	8.01E-03
14	8.232	1.45E-02	1.23E-02	1.09E-02	9.82E-03	8.86E-03	8.01E-03	7.45E-03	6.89E-03	7.38E-03
15	8.999	1.54E-02	1.31E-02	1.12E-02	1.00E-02	8.91E-03	7.97E-03	7.38E-03	6.62E-03	6.31E-03
16	9.776	1.72E-02	1.41E-02	1.14E-02	1.02E-02	9.18E-03	8.18E-03	7.42E-03	6.77E-03	6.31E-03
17	10.562	1.75E-02	1.51E-02	1.27E-02	1.09E-02	9.24E-03	8.38E-03	7.46E-03	6.87E-03	6.04E-03
18	11.357	1.56E-02	1.54E-02	1.41E-02	1.16E-02	9.76E-03	8.52E-03	7.58E-03	6.76E-03	6.18E-03
19	12.159	1.08E-02	1.39E-02	1.37E-02	1.28E-02	1.10E-02	9.00E-03	7.95E-03	6.95E-03	6.24E-03
20	12.968	2.64E-03	9.60E-03	1.24E-02	1.26E-02	1.17E-02	9.80E-03	8.59E-03	7.48E-03	6.41E-03
21	13.787	0.0	2.32E-03	8.42E-03	1.14E-02	1.13E-02	1.07E-02	9.27E-03	7.54E-03	6.72E-03
22	14.606	0.0	0.0	2.09E-03	7.62E-03	1.04E-02	1.02E-02	9.68E-03	8.12E-03	7.31E-03
23	15.436	0.0	0.0	0.0	1.89E-03	6.69E-03	9.31E-03	9.13E-03	8.90E-03	7.74E-03
24	16.266	0.0	0.0	0.0	0.0	1.74E-03	5.88E-03	8.58E-03	8.29E-03	8.00E-03
25	17.106	0.0	0.0	0.0	0.0	0.0	1.43E-03	5.20E-03	7.75E-03	7.84E-03
26	17.946	0.0	0.0	0.0	0.0	0.0	0.0	1.23E-03	4.68E-03	7.00E-03
27	18.795	0.0	0.0	0.0	0.0	0.0	0.0	0.0	1.13E-03	3.94E-03
28	19.641	0.0	0.0	0.0	0.0	0.0	0.0	0.0	0.0	1.02E-03
29	20.484	0.0	0.0	0.0	0.0	0.0	0.0	0.0	0.0	0.0
		Group No. 30 through 60 same as above								

Table 5 (continued)

Group No.	Light output [MeVee]	Upper Energy Boundary of Neutron Group [MeV] 28.0	29.0	30.0	31.0	32.0	33.0	34.0	35.0	36.0
1	0.196	2.67E-01	2.69E-01	2.78E-01	2.69E-01	2.67E-01	2.67E-01	2.65E-01	2.63E-01	2.63E-01
2	0.543	1.62E-02	1.50E-02	1.46E-02	1.39E-02	1.32E-02	1.17E-02	1.15E-02	1.09E-02	1.03E-02
3	0.983	1.61E-02	1.53E-02	1.45E-02	1.45E-02	1.38E-02	1.28E-02	1.25E-02	1.16E-02	1.07E-02
4	1.486	2.29E-02	2.20E-02	2.10E-02	2.02E-02	2.04E-02	1.94E-02	1.29E-02	1.26E-02	1.16E-02
5	2.037	2.28E-02	1.96E-02	1.82E-02	1.69E-02	1.63E-02	1.53E-02	1.38E-02	1.34E-02	1.30E-02
6	2.629	2.64E-02	2.32E-02	1.96E-02	1.65E-02	1.52E-02	1.39E-02	1.31E-02	1.27E-02	1.30E-02
7	3.256	2.16E-02	2.20E-02	2.08E-02	1.91E-02	1.69E-02	1.46E-02	1.39E-02	1.24E-02	1.27E-02
8	3.911	1.47E-02	1.57E-02	1.66E-02	1.64E-02	1.58E-02	1.45E-02	1.40E-02	1.37E-02	1.28E-02
9	4.590	1.30E-02	1.25E-02	1.26E-02	1.23E-02	1.25E-02	1.25E-02	1.22E-02	1.21E-02	1.21E-02
10	5.287	1.07E-02	1.11E-02	1.10E-02	1.07E-02	9.88E-03	9.94E-03	9.82E-03	1.04E-02	1.03E-02
11	6.002	1.02E-02	1.01E-02	9.66E-03	9.68E-03	9.99E-03	8.90E-03	8.80E-03	8.55E-03	9.29E-03
12	6.732	9.77E-03	9.68E-03	9.65E-03	9.33E-03	8.89E-03	8.48E-03	8.50E-03	8.30E-03	8.34E-03
13	7.476	7.88E-03	9.77E-03	9.63E-03	8.92E-03	8.55E-03	8.39E-03	7.86E-03	7.66E-03	7.85E-03
14	8.232	7.25E-03	7.35E-03	9.21E-03	8.73E-03	8.66E-03	8.08E-03	7.63E-03	7.53E-03	7.54E-03
15	8.999	6.80E-03	6.78E-03	6.77E-03	8.09E-03	8.53E-03	7.56E-03	7.62E-03	7.14E-03	7.48E-03
16	9.776	5.84E-03	6.33E-03	6.27E-03	5.96E-03	7.52E-03	8.05E-03	7.57E-03	7.29E-03	7.26E-03
17	10.562	5.60E-03	5.41E-03	5.99E-03	5.80E-03	5.49E-03	6.60E-03	7.91E-03	7.05E-03	7.56E-03
18	11.357	5.56E-03	5.34E-03	5.13E-03	5.77E-03	5.34E-03	5.15E-03	6.11E-03	7.21E-03	7.45E-03
19	12.159	5.52E-03	5.27E-03	4.86E-03	4.90E-03	5.29E-03	5.14E-03	4.58E-03	5.41E-03	6.96E-03
20	12.968	5.67E-03	5.28E-03	4.84E-03	4.53E-03	4.57E-03	4.80E-03	4.54E-03	4.42E-03	5.06E-03
21	13.787	6.06E-03	5.45E-03	5.15E-03	4.50E-03	4.23E-03	4.02E-03	4.16E-03	4.32E-03	4.15E-03
22	14.606	6.19E-03	5.70E-03	5.06E-03	4.71E-03	4.21E-03	3.98E-03	3.72E-03	4.00E-03	4.06E-03
23	15.436	6.69E-03	5.69E-03	5.33E-03	4.70E-03	4.29E-03	3.84E-03	3.65E-03	3.60E-03	3.81E-03
24	16.266	7.06E-03	6.16E-03	5.58E-03	4.80E-03	4.50E-03	4.17E-03	3.62E-03	3.48E-03	3.42E-03
25	17.106	7.36E-03	6.76E-03	5.83E-03	5.02E-03	4.74E-03	4.35E-03	3.66E-03	3.48E-03	3.32E-03
26	17.946	6.90E-03	6.77E-03	6.15E-03	5.57E-03	4.95E-03	4.35E-03	3.77E-03	3.59E-03	3.25E-03
27	18.795	6.37E-03	6.75E-03	6.37E-03	6.02E-03	4.93E-03	4.45E-03	3.87E-03	3.64E-03	3.38E-03
28	19.641	3.37E-03	5.89E-03	6.33E-03	5.81E-03	5.58E-03	4.54E-03	4.09E-03	3.74E-03	3.39E-03
29	20.484	8.82E-04	3.13E-03	5.57E-03	5.57E-03	5.29E-03	4.95E-03	4.34E-03	3.93E-03	3.53E-03
30	21.329	0.0	8.64E-04	2.84E-03	4.74E-03	5.32E-03	4.91E-03	4.59E-03	4.16E-03	3.71E-03
31	22.177	0.0	0.0	7.03E-04	2.58E-03	4.42E-03	4.78E-03	4.65E-03	4.39E-03	3.90E-03
32	23.026	0.0	0.0	0.0	6.55E-04	2.12E-03	4.08E-03	4.57E-03	4.39E-03	4.14E-03
33	23.875	0.0	0.0	0.0	0.0	5.89E-04	2.11E-03	4.00E-03	4.32E-03	4.17E-03
34	24.727	0.0	0.0	0.0	0.0	0.0	4.91E-04	2.47E-03	3.84E-03	4.14E-03
35	25.577	0.0	0.0	0.0	0.0	0.0	0.0	9.71E-04	2.42E-03	3.66E-03
36	26.426	0.0	0.0	0.0	0.0	0.0	0.0	0.0	9.84E-04	2.30E-03
37	27.274	0.0	0.0	0.0	0.0	0.0	0.0	0.0	0.0	9.30E-04
38	28.120	0.0	0.0	0.0	0.0	0.0	0.0	0.0	0.0	0.0
		Group No. 39 through 60 same as above								

Table 5 (continued)

Group No.	Upper Light [MeVee]	Upper Energy Boundary of Neutron Group [MeV] 37.0	38.0	39.0	40.0	41.0	42.0	43.0	44.0	46.0
1	0.196	2.60E-01	2.59E-01	2.58E-01	2.56E-01	2.54E-01	2.52E-01	2.50E-01	2.48E-01	2.44E-01
2	0.543	9.48E-03	8.89E-03	7.90E-03	8.51E-03	7.78E-03	7.61E-03	7.09E-03	7.12E-03	6.46E-03
3	0.983	1.03E-02	9.36E-03	8.80E-03	9.14E-03	8.57E-03	8.74E-03	7.99E-03	7.86E-03	7.32E-03
4	1.486	1.14E-02	1.03E-02	9.77E-03	9.17E-03	8.78E-03	8.45E-03	8.11E-03	7.91E-03	7.35E-03
5	2.037	1.26E-02	1.17E-02	1.15E-02	1.06E-02	1.05E-02	9.22E-03	8.92E-03	8.15E-03	7.50E-03
6	2.629	1.30E-02	1.21E-02	1.28E-02	1.17E-02	1.11E-02	1.08E-02	1.04E-02	9.75E-03	8.89E-03
7	3.256	1.18E-02	1.12E-02	1.17E-02	1.13E-02	1.12E-02	1.14E-02	1.04E-02	9.93E-03	9.19E-03
8	3.911	1.18E-02	1.12E-02	1.05E-02	1.04E-02	1.03E-02	1.00E-02	9.65E-03	9.34E-03	9.00E-03
9	4.590	1.18E-02	1.11E-02	1.13E-02	1.03E-02	9.52E-03	9.21E-03	8.99E-03	8.74E-03	8.33E-03
10	5.287	1.03E-02	1.01E-02	1.08E-02	1.03E-02	9.65E-03	9.35E-03	8.08E-03	8.09E-03	7.70E-03
11	6.002	8.91E-03	8.43E-03	8.99E-03	8.89E-03	9.13E-03	8.69E-03	8.41E-03	8.19E-03	7.42E-03
12	6.732	7.57E-03	7.20E-03	8.01E-03	7.81E-03	8.13E-03	7.95E-03	8.02E-03	8.03E-03	7.45E-03
13	7.476	7.53E-03	7.09E-03	6.96E-03	6.40E-03	6.74E-03	6.86E-03	6.94E-03	7.14E-03	7.12E-03
14	8.232	7.38E-03	6.75E-03	6.84E-03	6.29E-03	6.07E-03	6.08E-03	6.00E-03	6.20E-03	6.47E-03
15	8.999	6.72E-03	6.33E-03	6.65E-03	6.71E-03	5.86E-03	6.00E-03	5.41E-03	5.37E-03	5.71E-03
16	9.776	6.90E-03	6.53E-03	6.23E-03	6.16E-03	5.82E-03	5.73E-03	5.46E-03	5.18E-03	5.17E-03
17	10.562	6.80E-03	6.20E-03	6.43E-03	5.94E-03	5.63E-03	5.10E-03	5.21E-03	5.02E-03	4.72E-03
18	11.357	6.76E-03	6.46E-03	6.12E-03	5.77E-03	5.43E-03	5.66E-03	5.05E-03	5.10E-03	4.51E-03
19	12.159	6.58E-03	6.32E-03	6.02E-03	5.61E-03	5.46E-03	5.10E-03	4.75E-03	4.48E-03	4.15E-03
20	12.968	6.35E-03	6.49E-03	6.24E-03	5.66E-03	5.46E-03	5.26E-03	4.68E-03	4.37E-03	4.15E-03
21	13.787	4.66E-03	6.28E-03	6.43E-03	5.87E-03	5.45E-03	5.31E-03	4.79E-03	4.53E-03	4.18E-03
22	14.606	3.75E-03	4.40E-03	5.92E-03	6.15E-03	5.82E-03	5.35E-03	4.96E-03	4.61E-03	4.17E-03
23	15.436	3.79E-03	3.68E-03	4.20E-03	5.53E-03	6.16E-03	5.66E-03	5.15E-03	4.65E-03	4.27E-03
24	16.266	3.53E-03	3.58E-03	3.45E-03	3.86E-03	5.32E-03	5.80E-03	5.34E-03	4.92E-03	4.44E-03
25	17.106	3.15E-03	3.42E-03	3.53E-03	3.29E-03	3.65E-03	4.99E-03	5.64E-03	5.20E-03	4.62E-03
26	17.946	2.96E-03	3.08E-03	3.28E-03	3.28E-03	3.17E-03	3.51E-03	4.61E-03	5.31E-03	4.86E-03
27	18.795	3.06E-03	2.85E-03	3.00E-03	3.07E-03	3.08E-03	3.00E-03	3.27E-03	4.19E-03	4.99E-03
28	19.641	3.00E-03	2.92E-03	2.82E-03	2.79E-03	2.87E-03	2.97E-03	2.77E-03	2.97E-03	4.38E-03
29	20.484	3.11E-03	2.94E-03	2.78E-03	2.59E-03	2.61E-03	2.77E-03	2.69E-03	2.57E-03	3.26E-03
30	21.329	3.27E-03	3.02E-03	2.81E-03	2.61E-03	2.46E-03	2.49E-03	2.58E-03	2.56E-03	2.55E-03
31	22.177	3.41E-03	3.16E-03	2.92E-03	2.69E-03	2.52E-03	2.37E-03	2.31E-03	2.38E-03	2.40E-03
32	23.026	3.65E-03	3.31E-03	3.02E-03	2.69E-03	2.45E-03	2.38E-03	2.21E-03	2.21E-03	2.40E-03
33	23.875	3.83E-03	3.44E-03	3.16E-03	2.78E-03	2.61E-03	2.42E-03	2.13E-03	2.11E-03	2.16E-03
34	24.727	3.81E-03	3.68E-03	3.31E-03	2.98E-03	2.71E-03	2.56E-03	2.23E-03	2.06E-03	2.01E-03
35	25.577	3.81E-03	3.64E-03	3.45E-03	3.18E-03	2.93E-03	2.62E-03	2.38E-03	2.13E-03	1.91E-03
36	26.426	3.34E-03	3.57E-03	3.50E-03	3.10E-03	2.94E-03	2.72E-03	2.39E-03	2.14E-03	1.93E-03
37	27.274	2.07E-03	3.20E-03	3.49E-03	3.27E-03	3.07E-03	2.78E-03	2.42E-03	2.24E-03	2.01E-03
38	28.120	8.64E-04	1.96E-03	3.05E-03	3.22E-03	3.13E-03	2.89E-03	2.63E-03	2.33E-03	2.01E-03
39	28.966	0.0	8.34E-04	1.85E-03	2.74E-03	3.11E-03	2.96E-03	2.65E-03	2.47E-03	2.08E-03
40	29.809	0.0	0.0	7.82E-04	1.74E-03	2.67E-03	2.98E-03	2.71E-03	2.52E-03	2.18E-03
41	30.651	0.0	0.0	0.0	7.73E-04	1.63E-03	2.46E-03	2.76E-03	2.54E-03	2.30E-03
42	31.491	0.0	0.0	0.0	0.0	7.25E-04	1.53E-03	2.31E-03	2.57E-03	2.38E-03
43	32.328	0.0	0.0	0.0	0.0	0.0	7.12E-04	1.50E-03	2.15E-03	2.31E-03
44	33.162	0.0	0.0	0.0	0.0	0.0	0.0	6.38E-04	1.35E-03	2.15E-03
45	34.822	0.0	0.0	0.0	0.0	0.0	0.0	0.0	8.31E-04	2.42E-03
46	36.473	0.0	0.0	0.0	0.0	0.0	0.0	0.0	0.0	5.03E-04
47	38.113	0.0	0.0	0.0	0.0	0.0	0.0	0.0	0.0	0.0
		Group No. 48 through 60 same as above								

Table 5 (continued)

Group No.	Upper Light [MeVee]	Upper Energy Boundary of Neutron Group [MeV] 48.0	50.0	52.0	54.0	56.0	58.0	60.0	62.0	64.0
1	0.196	2.36E-01	2.28E-01	2.22E-01	2.19E-01	2.15E-01	2.09E-01	2.03E-01	1.97E-01	1.92E-01
2	0.543	5.81E-03	5.61E-03	5.22E-03	5.01E-03	4.69E-03	4.42E-03	4.09E-03	3.94E-03	3.97E-03
3	0.983	6.63E-03	6.24E-03	5.86E-03	5.39E-03	5.14E-03	4.93E-03	4.43E-03	4.32E-03	4.24E-03
4	1.486	6.74E-03	6.58E-03	5.90E-03	5.54E-03	5.34E-03	5.15E-03	4.67E-03	4.56E-03	4.52E-03
5	2.037	6.78E-03	6.38E-03	5.80E-03	5.41E-03	5.25E-03	4.88E-03	4.70E-03	4.50E-03	4.29E-03
6	2.629	8.42E-03	7.42E-03	6.52E-03	5.88E-03	5.66E-03	3.84E-03	4.71E-03	4.43E-03	4.05E-03
7	3.256	8.47E-03	7.24E-03	6.73E-03	5.87E-03	5.75E-03	5.14E-03	4.71E-03	4.38E-03	3.92E-03
8	3.911	8.81E-03	7.29E-03	6.34E-03	5.86E-03	5.64E-03	5.20E-03	4.78E-03	4.36E-03	4.04E-03
9	4.590	8.16E-03	7.22E-03	6.40E-03	5.79E-03	5.49E-03	5.00E-03	4.63E-03	4.27E-03	3.81E-03
10	5.287	7.65E-03	6.98E-03	6.11E-03	5.82E-03	5.45E-03	4.97E-03	4.52E-03	4.05E-03	3.67E-03
11	6.002	7.48E-03	6.37E-03	5.67E-03	5.23E-03	5.29E-03	5.26E-03	4.34E-03	3.90E-03	3.64E-03
12	6.732	6.84E-03	6.16E-03	5.56E-03	5.46E-03	5.27E-03	4.87E-03	4.08E-03	3.75E-03	3.48E-03
13	7.476	6.95E-03	5.87E-03	5.58E-03	5.10E-03	5.17E-03	5.17E-03	4.35E-03	3.85E-03	3.50E-03
14	8.232	6.43E-03	5.95E-03	5.21E-03	5.11E-03	4.73E-03	4.83E-03	4.29E-03	3.88E-03	3.43E-03
15	8.999	6.19E-03	5.58E-03	5.19E-03	4.50E-03	4.62E-03	4.34E-03	4.27E-03	3.88E-03	3.28E-03
16	9.776	5.25E-03	5.20E-03	4.85E-03	4.81E-03	4.37E-03	4.44E-03	4.13E-03	3.74E-03	3.28E-03
17	10.562	5.17E-03	4.78E-03	4.75E-03	4.79E-03	4.83E-03	4.33E-03	3.73E-03	3.60E-03	3.35E-03
18	11.357	4.57E-03	4.27E-03	4.39E-03	4.03E-03	4.18E-03	4.35E-03	3.78E-03	3.51E-03	3.29E-03
19	12.159	4.13E-03	3.94E-03	3.95E-03	3.92E-03	4.04E-03	3.71E-03	3.69E-03	3.45E-03	3.26E-03
20	12.968	3.84E-03	3.70E-03	3.68E-03	3.51E-03	3.64E-03	3.57E-03	3.61E-03	3.37E-03	3.14E-03
21	13.787	3.83E-03	3.41E-03	3.47E-03	3.39E-03	3.43E-03	3.53E-03	3.53E-03	3.24E-03	3.10E-03
22	14.606	3.80E-03	3.35E-03	3.25E-03	3.26E-03	3.26E-03	3.27E-03	3.25E-03	3.11E-03	2.94E-03
23	15.436	3.90E-03	3.41E-03	3.08E-03	3.12E-03	3.19E-03	3.09E-03	3.11E-03	3.17E-03	2.98E-03
24	16.266	3.94E-03	3.30E-03	3.07E-03	2.85E-03	2.92E-03	3.03E-03	3.03E-03	2.89E-03	2.88E-03
25	17.106	4.09E-03	3.36E-03	3.13E-03	2.81E-03	2.74E-03	2.81E-03	3.09E-03	2.84E-03	2.67E-03
26	17.946	4.21E-03	3.55E-03	3.07E-03	2.82E-03	2.71E-03	2.75E-03	2.76E-03	2.78E-03	2.53E-03
27	18.795	4.36E-03	3.53E-03	3.16E-03	2.79E-03	2.65E-03	2.65E-03	2.59E-03	2.63E-03	2.49E-03
28	19.641	4.63E-03	3.70E-03	3.31E-03	2.92E-03	2.57E-03	2.37E-03	2.42E-03	2.59E-03	2.38E-03
29	20.484	4.59E-03	3.98E-03	3.24E-03	2.75E-03	2.63E-03	2.39E-03	2.16E-03	2.31E-03	2.24E-03
30	21.329	3.99E-03	4.18E-03	3.49E-03	2.79E-03	2.52E-03	2.43E-03	2.23E-03	2.21E-03	2.16E-03
31	22.177	2.98E-03	4.10E-03	3.74E-03	2.96E-03	2.65E-03	2.38E-03	2.42E-03	1.99E-03	2.12E-03
32	23.026	2.40E-03	3.52E-03	3.98E-03	3.32E-03	2.69E-03	2.41E-03	2.24E-03	2.13E-03	1.99E-03
33	23.875	2.26E-03	2.56E-03	3.84E-03	3.46E-03	2.85E-03	2.42E-03	2.23E-03	1.93E-03	1.79E-03
34	24.727	2.13E-03	1.98E-03	3.17E-03	3.69E-03	3.13E-03	2.46E-03	2.36E-03	2.00E-03	1.90E-03
35	25.577	1.97E-03	1.91E-03	2.33E-03	3.34E-03	3.38E-03	2.71E-03	2.30E-03	2.03E-03	1.75E-03
36	26.426	1.80E-03	1.85E-03	1.94E-03	2.70E-03	3.48E-03	2.84E-03	2.35E-03	2.11E-03	1.77E-03
37	27.274	1.78E-03	1.75E-03	1.76E-03	2.05E-03	3.20E-03	3.18E-03	2.63E-03	2.15E-03	1.85E-03
38	28.120	1.70E-03	1.60E-03	1.72E-03	1.63E-03	2.50E-03	3.13E-03	2.72E-03	2.28E-03	1.86E-03
39	28.966	1.81E-03	1.48E-03	1.58E-03	1.58E-03	1.83E-03	2.90E-03	2.99E-03	2.20E-03	2.01E-03
40	29.809	1.86E-03	1.51E-03	1.45E-03	1.51E-03	1.59E-03	2.30E-03	3.01E-03	2.60E-03	2.03E-03
41	30.651	2.00E-03	1.58E-03	1.42E-03	1.40E-03	1.48E-03	1.61E-03	2.34E-03	2.75E-03	2.18E-03
42	31.491	2.04E-03	1.64E-03	1.40E-03	1.27E-03	1.35E-03	1.42E-03	1.70E-03	2.51E-03	2.41E-03
43	32.328	2.15E-03	1.65E-03	1.37E-03	1.26E-03	1.28E-03	1.41E-03	1.28E-03	1.99E-03	2.48E-03
44	33.162	2.15E-03	1.78E-03	1.49E-03	1.28E-03	1.19E-03	1.31E-03	1.22E-03	1.35E-03	2.19E-03
45	34.822	4.03E-03	3.72E-03	3.14E-03	2.52E-03	2.26E-03	2.26E-03	2.27E-03	2.23E-03	2.90E-03
46	36.473	2.24E-03	3.50E-03	3.28E-03	2.74E-03	2.34E-03	2.14E-03	2.09E-03	1.98E-03	2.12E-03
47	38.113	4.85E-04	1.92E-03	3.20E-03	2.98E-03	2.55E-03	2.13E-03	1.92E-03	1.81E-03	1.88E-03
48	39.742	0.0	4.43E-04	1.73E-03	2.88E-03	2.75E-03	2.36E-03	1.98E-03	1.69E-03	1.46E-03
49	41.365	0.0	0.0	3.95E-04	1.53E-03	2.61E-03	2.57E-03	2.15E-03	1.79E-03	1.56E-03
50	42.983	0.0	0.0	0.0	3.57E-04	1.41E-03	2.32E-03	2.23E-03	1.93E-03	1.60E-03
51	44.592	0.0	0.0	0.0	0.0	3.12E-04	1.23E-03	2.10E-03	2.00E-03	1.83E-03
52	46.194	0.0	0.0	0.0	0.0	0.0	2.51E-04	1.08E-03	2.01E-03	1.79E-03
53	47.788	0.0	0.0	0.0	0.0	0.0	0.0	2.07E-04	9.47E-04	1.72E-03
54	49.372	0.0	0.0	0.0	0.0	0.0	0.0	0.0	2.50E-04	8.56E-04
55	50.948	0.0	0.0	0.0	0.0	0.0	0.0	0.0	0.0	2.03E-04
56	52.518	0.0	0.0	0.0	0.0	0.0	0.0	0.0	0.0	0.0
		Group No. 57 through 60 same as above								

Table 5 (continued)

Group No.	Upper Light [MeVee]	Upper Energy Boundary of Neutron Group [MeV] 66.0	68.0	70.0	74.0	78.0
1	0.196	1.87E-01	1.82E-01	1.78E-01	1.70E-01	1.62E-01
2	0.543	3.70E-03	3.53E-03	3.42E-03	3.28E-03	3.02E-03
3	0.983	3.98E-03	3.48E-03	3.52E-03	3.20E-03	3.01E-03
4	1.486	4.05E-03	3.77E-03	3.70E-03	3.29E-03	3.16E-03
5	2.037	4.05E-03	3.75E-03	3.74E-03	3.23E-03	2.99E-03
6	2.629	3.95E-03	3.65E-03	3.57E-03	3.30E-03	3.13E-03
7	3.256	3.78E-03	3.72E-03	3.34E-03	3.14E-03	2.69E-03
8	3.911	3.83E-03	3.76E-03	3.53E-03	3.17E-03	2.70E-03
9	4.590	3.78E-03	3.74E-03	3.71E-03	3.43E-03	2.97E-03
10	5.287	3.77E-03	3.53E-03	3.50E-03	3.23E-03	2.80E-03
11	6.002	3.58E-03	3.36E-03	3.52E-03	3.22E-03	2.72E-03
12	6.732	3.54E-03	3.24E-03	3.42E-03	3.14E-03	2.49E-03
13	7.476	3.44E-03	3.39E-03	3.40E-03	3.07E-03	2.64E-03
14	8.232	3.37E-03	3.20E-03	3.28E-03	3.05E-03	2.51E-03
15	8.999	3.27E-03	3.30E-03	3.23E-03	2.95E-03	2.50E-03
16	9.776	3.30E-03	3.15E-03	3.30E-03	2.98E-03	2.47E-03
17	10.562	3.44E-03	3.04E-03	3.30E-03	2.90E-03	2.33E-03
18	11.357	3.29E-03	3.26E-03	3.11E-03	2.90E-03	2.41E-03
19	12.159	3.21E-03	3.22E-03	3.34E-03	2.79E-03	2.32E-03
20	12.968	3.19E-03	3.14E-03	3.11E-03	2.73E-03	2.34E-03
21	13.787	2.98E-03	2.94E-03	3.10E-03	2.73E-03	2.34E-03
22	14.606	2.94E-03	2.89E-03	3.08E-03	2.73E-03	2.36E-03
23	15.436	2.86E-03	3.05E-03	3.10E-03	2.67E-03	2.22E-03
24	16.266	2.83E-03	2.91E-03	2.85E-03	2.63E-03	2.25E-03
25	17.106	2.78E-03	2.74E-03	2.70E-03	2.53E-03	2.17E-03
26	17.946	2.67E-03	2.75E-03	2.79E-03	2.56E-03	2.18E-03
27	18.795	2.56E-03	2.77E-03	2.75E-03	2.59E-03	2.18E-03
28	19.641	2.54E-03	2.42E-03	2.70E-03	2.42E-03	2.09E-03
29	20.484	2.45E-03	2.30E-03	2.42E-03	2.38E-03	2.01E-03
30	21.329	2.36E-03	2.30E-03	2.50E-03	2.32E-03	2.11E-03
31	22.177	2.08E-03	2.08E-03	2.44E-03	2.33E-03	2.00E-03
32	23.026	2.04E-03	2.17E-03	2.31E-03	2.18E-03	1.98E-03
33	23.875	2.04E-03	2.08E-03	2.26E-03	2.03E-03	1.87E-03
34	24.727	1.80E-03	1.80E-03	2.15E-03	1.93E-03	1.80E-03
35	25.577	1.77E-03	1.78E-03	2.03E-03	1.92E-03	1.68E-03
36	26.426	1.92E-03	1.84E-03	2.07E-03	1.80E-03	1.63E-03
37	27.274	1.78E-03	1.67E-03	1.83E-03	1.78E-03	1.62E-03
38	28.120	1.74E-03	1.74E-03	1.74E-03	1.74E-03	1.53E-03
39	28.966	1.73E-03	1.67E-03	1.72E-03	1.60E-03	1.60E-03
40	29.809	1.80E-03	1.68E-03	1.76E-03	1.55E-03	1.53E-03
41	30.651	1.94E-03	1.66E-03	1.57E-03	1.48E-03	1.46E-03
42	31.491	2.07E-03	1.76E-03	1.70E-03	1.48E-03	1.37E-03
43	32.328	2.26E-03	1.78E-03	1.77E-03	1.37E-03	1.32E-03
44	33.162	2.41E-03	1.83E-03	1.64E-03	1.36E-03	1.31E-03
45	34.822	4.57E-03	4.29E-03	3.68E-03	2.91E-03	2.41E-03
46	36.473	2.83E-03	4.07E-03	4.52E-03	3.02E-03	2.22E-03
47	38.113	1.98E-03	2.56E-03	3.97E-03	3.57E-03	2.25E-03
48	39.742	1.83E-03	1.91E-03	2.65E-03	3.57E-03	2.46E-03
49	41.365	1.58E-03	1.58E-03	1.85E-03	2.77E-03	2.85E-03
50	42.983	1.47E-03	1.45E-03	1.62E-03	1.85E-03	2.90E-03
51	44.592	1.57E-03	1.32E-03	1.39E-03	1.48E-03	2.11E-03
52	46.194	1.59E-03	1.53E-03	1.22E-03	1.32E-03	1.42E-03
53	47.788	1.72E-03	1.49E-03	1.39E-03	1.19E-03	1.18E-03
54	49.372	1.59E-03	1.58E-03	1.46E-03	1.21E-03	1.04E-03
55	50.948	7.69E-04	1.49E-03	1.55E-03	1.28E-03	1.01E-03
56	52.518	1.72E-04	7.62E-04	1.44E-03	1.27E-03	9.18E-04
57	54.079	0.0	1.62E-04	7.63E-04	1.29E-03	9.72E-04
58	57.171	0.0	0.0	2.17E-04	1.35E-03	2.16E-03
59	60.225	0.0	0.0	0.0	1.30E-04	1.04E-03
60	63.249	0.0	0.0	0.0	0.0	9.24E-05

Table 6 Response functions of Bonner ball detector.

Upper Energy Boundary [eV]	Response [counts neutron^{-1} cm^2]					
	Bare [a]	1.5cm [b]	1.5cm+Cd [c]	3.0cm	5.0cm	9.0cm
4.00E+08 [d]	0.000E+00	7.500E-03	1.212E-01	6.624E-02	2.465E-01	7.141E-01
3.50E+08	0.000E+00	7.603E-03	1.204E-01	6.710E-02	2.492E-01	7.189E-01
3.00E+08	0.000E+00	8.210E-03	1.168E-01	7.326E-02	2.737E-01	7.905E-01
2.50E+08	0.000E+00	8.831E-03	1.131E-01	7.866E-02	2.934E-01	8.440E-01
2.00E+08	0.000E+00	9.648E-03	1.110E-01	8.484E-02	3.132E-01	8.910E-01
1.60E+08	0.000E+00	1.110E-02	1.090E-01	9.654E-02	3.529E-01	9.907E-01
1.20E+08	0.000E+00	1.280E-02	1.072E-01	1.104E-01	3.998E-01	1.107E+00
1.00E+08	0.000E+00	1.425E-02	1.072E-01	1.226E-01	4.425E-01	1.216E+00
8.00E+07	0.000E+00	1.565E-02	1.069E-01	1.349E-01	4.868E-01	1.332E+00
6.50E+07	0.000E+00	1.702E-02	1.049E-01	1.468E-01	5.296E-01	1.443E+00
5.50E+07	0.000E+00	1.809E-02	1.024E-01	1.560E-01	5.623E-01	1.527E+00
4.50E+07	0.000E+00	1.957E-02	1.018E-01	1.690E-01	6.106E-01	1.658E+00
3.50E+07	3.089E-03	2.312E-02	1.185E-01	1.995E-01	7.198E-01	1.941E+00
2.75E+07	7.928E-03	2.808E-02	1.154E-01	2.409E-01	8.650E-01	2.298E+00
2.25E+07	1.133E-02	3.749E-02	1.284E-01	3.165E-01	1.115E+00	2.856E+00
1.75E+07	1.730E-02	5.766E-02	1.396E-01	4.246E-01	1.438E+00	3.486E+00
1.35E+07	2.313E-02	8.420E-02	1.263E-01	5.348E-01	1.758E+00	4.099E+00
1.00E+07	3.072E-02	1.239E-01	1.541E-01	7.926E-01	2.498E+00	5.327E+00
6.70E+06	3.902E-02	2.010E-01	2.399E-01	1.273E+00	3.721E+00	6.945E+00
4.49E+06	4.692E-02	3.001E-01	3.509E-01	1.830E+00	4.882E+00	7.672E+00
3.01E+06	5.285E-02	4.456E-01	5.126E-01	2.587E+00	6.317E+00	8.514E+00
2.02E+06	5.474E-02	6.413E-01	7.286E-01	3.482E+00	7.721E+00	8.768E+00
1.35E+06	3.315E-02	8.836E-01	9.762E-01	4.420E+00	8.785E+00	8.184E+00
9.07E+05	1.558E-02	1.276E+00	1.387E+00	5.539E+00	9.560E+00	6.953E+00
4.98E+05	1.831E-02	1.941E+00	2.084E+00	6.808E+00	9.768E+00	5.165E+00
2.24E+05	2.814E-02	2.779E+00	2.922E+00	7.765E+00	9.243E+00	3.613E+00
8.65E+04	6.642E-02	3.874E+00	3.949E+00	8.481E+00	8.393E+00	2.574E+00
1.50E+04	1.616E-01	5.194E+00	5.175E+00	9.251E+00	7.861E+00	2.044E+00
3.35E+03	4.011E-01	6.778E+00	6.596E+00	1.001E+01	7.479E+00	1.740E+00
4.54E+02	1.572E+00	9.425E+00	8.548E+00	1.066E+01	6.709E+00	1.381E+00
2.26E+01	4.537E+00	1.208E+01	1.171E+01	1.040E+01	5.536E+00	1.036E+00
5.04E+00	9.596E+00	1.275E+01	1.239E+01	9.083E+00	4.437E+00	8.043E-01
1.12E+00	1.759E+01	1.143E+01	7.941E+00	6.992E+00	3.254E+00	5.812E-01
4.14E-01	1.881E+01	4.797E+00	1.300E-02	2.607E+00	1.190E+00	2.193E-01
1.00E-04						

a ^{3}He counter (10 atm)

b Thickness of polyethylene moderator

c 1.5-cm thick polyethylene moderator covered with 1mm thick Cd thermal neutron absorbor

d Read as 4.00 x 10^8

Table 7 Fission cross sections of ^{232}Th and ^{238}U.

Upper Energy Boundary [eV]	Cross Section [b]		Upper Energy Boundary [eV]	Cross Section [b]	
	^{232}Th	^{238}U		^{232}Th	^{238}U
4.00E+08*	5.7915E-01	1.3016E+00	1.22E+07	3.1267E-01	9.7859E-01
3.75E+08	6.6380E-01	1.3128E+00	1.00E+07	3.3698E-01	9.9039E-01
3.50E+08	7.4080E-01	1.3296E+00	8.19E+06	3.8746E-01	9.7573E-01
3.25E+08	7.6801E-01	1.3394E+00	6.70E+06	1.9931E-01	6.5639E-01
3.00E+08	7.8376E-01	1.3434E+00	5.49E+06	1.4968E-01	5.3713E-01
2.75E+08	8.0047E-01	1.3334E+00	4.49E+06	1.4624E-01	5.6118E-01
2.50E+08	8.0915E-01	1.3254E+00	3.68E+06	1.4599E-01	5.3383E-01
2.25E+08	8.1796E-01	1.3224E+00	3.01E+06	1.2797E-01	5.3862E-01
2.00E+08	7.3489E-01	1.3244E+00	2.46E+06	1.2712E-01	5.4919E-01
1.80E+08	7.7471E-01	1.3194E+00	2.02E+06	1.0315E-01	4.9559E-01
1.60E+08	7.5311E-01	1.3227E+00	1.65E+06	8.3819E-02	3.1461E-01
1.40E+08	8.0410E-01	1.3516E+00	1.35E+06	1.3551E-02	5.1671E-02
1.20E+08	7.8314E-01	1.3583E+00	1.11E+06	1.7806E-03	1.8998E-02
1.10E+08	8.0839E-01	1.4180E+00	9.07E+05	5.9640E-04	6.5292E-03
1.00E+08	8.4285E-01	1.4493E+00	7.43E+05	1.1990E-04	1.0334E-03
9.00E+07	8.6533E-01	1.4845E+00	4.98E+05	1.2951E-05	2.5770E-04
8.00E+07	8.7328E-01	1.5234E+00	3.34E+05	0.0000E+00	9.6159E-05
7.00E+07	8.9851E-01	1.5383E+00	2.24E+05	0.0000E+00	9.9000E-05
6.50E+07	9.0406E-01	1.5893E+00	1.50E+05	0.0000E+00	3.9529E-05
6.00E+07	8.7216E-01	1.6395E+00	8.65E+04	0.0000E+00	6.1295E-05
5.50E+07	7.9173E-01	1.6442E+00	3.18E+04	0.0000E+00	9.6385E-05
5.00E+07	8.2978E-01	1.6656E+00	1.50E+04	0.0000E+00	1.1010E-04
4.50E+07	8.3477E-01	1.6856E+00	7.10E+03	0.0000E+00	6.7200E-06
4.00E+07	7.8467E-01	1.6738E+00	3.35E+03	0.0000E+00	4.0000E-08
3.50E+07	7.5686E-01	1.6621E+00	1.58E+03	0.0000E+00	4.5624E-08
3.00E+07	6.5461E-01	1.6173E+00	4.54E+02	0.0000E+00	8.7118E-08
2.75E+07	6.4635E-01	1.5813E+00	1.01E+02	0.0000E+00	1.8165E-07
2.50E+07	6.4801E-01	1.5717E+00	2.26E+01	0.0000E+00	3.0957E-07
2.25E+07	5.8063E-01	1.4748E+00	1.07E+01	0.0000E+00	4.4716E-07
1.96E+07	5.0863E-01	1.2133E+00	5.04E+00	0.0000E+00	6.4625E-07
1.75E+07	4.4226E-01	1.2344E+00	2.38E+00	0.0000E+00	9.3423E-07
1.49E+07	3.7120E-01	1.1358E+00	1.12E+00	0.0000E+00	1.4397E-06
1.35E+07	3.1923E-01	1.0034E+00	4.14E-01	0.0000E+00	6.3656E-06

* Read as 4.00 x 10^8
Lowest energy boundary is 1.00E-04 [eV]

Table 8 Calculated responses of ^{7}LiF and ^{nat}LiF TLDs.

Energy [MeV]	Response [^{60}Co-eq. R cm^2]		Energy [MeV]	Response [^{60}Co-eq. R cm^2]		Energy [MeV]	Response [^{60}Co-eq. R cm^2]	
	^{7}LiF	^{nat}LiF		^{7}LiF	^{nat}LiF		^{7}LiF	^{nat}LiF
1.649E+01*	6.450E-10	6.800E-10	9.804E-02	1.077E-11	4.642E-11	2.902E-05	1.722E-12	1.287E-09
1.455E+01	5.662E-10	5.988E-10	8.652E-02	9.631E-12	4.419E-11	2.260E-05	1.949E-12	1.459E-09
1.284E+01	5.662E-10	5.988E-10	7.635E-02	5.039E-12	3.933E-11	1.760E-05	2.208E-12	1.653E-09
1.133E+01	5.204E-10	5.533E-10	6.738E-02	3.437E-12	3.802E-11	1.371E-05	2.501E-12	1.874E-09
1.000E+01	4.688E-10	5.028E-10	5.946E-02	2.820E-12	3.813E-11	1.068E-05	2.834E-12	2.124E-09
8.825E+00	4.099E-10	4.437E-10	5.946E-02	2.806E-12	3.917E-11	8.315E-06	3.211E-12	2.407E-09
7.788E+00	3.442E-10	3.767E-10	5.248E-02	2.806E-12	3.917E-11	6.476E-06	3.638E-12	2.727E-09
6.873E+00	2.990E-10	3.290E-10	4.631E-02	5.361E-12	4.302E-11	5.044E-06	4.122E-12	3.090E-09
6.065E+00	2.530E-10	2.804E-10	4.087E-02	2.579E-12	4.182E-11	3.928E-06	4.671E-12	3.502E-09
5.353E+00	2.186E-10	2.438E-10	3.607E-02	2.136E-12	4.319E-11	3.059E-06	5.292E-12	3.968E-09
4.724E+00	1.719E-10	1.949E-10	3.183E-02	1.709E-12	4.478E-11	2.382E-06	5.997E-12	4.497E-09
4.169E+00	1.543E-10	1.751E-10	2.809E-02	1.787E-12	4.710E-11	1.855E-06	6.798E-12	5.097E-09
3.679E+00	1.311E-10	1.500E-10	2.479E-02	3.036E-12	5.080E-11	1.445E-06	7.700E-12	5.774E-09
3.247E+00	1.218E-10	1.387E-10	2.187E-02	1.440E-12	5.188E-11	1.125E-06	8.728E-12	6.545E-09
2.865E+00	1.167E-10	1.315E-10	1.931E-02	1.141E-12	5.447E-11	8.764E-07	9.887E-12	7.414E-09
2.528E+00	1.152E-10	1.296E-10	1.704E-02	1.008E-12	5.742E-11	6.826E-07	1.120E-11	8.402E-09
2.231E+00	1.036E-10	1.194E-10	1.503E-02	9.274E-13	6.068E-11	5.316E-07	1.270E-11	9.523E-09
1.969E+00	9.057E-11	1.079E-10	1.171E-02	8.537E-13	6.615E-11	4.140E-07	1.438E-11	1.078E-08
1.738E+00	7.836E-11	9.669E-11	9.119E-03	6.922E-13	7.420E-11	1.518E-07	1.987E-11	1.490E-08
1.533E+00	7.452E-11	9.239E-11	7.102E-03	5.449E-13	8.350E-11	3.524E-10	3.417E-11	2.562E-08
1.353E+00	6.543E-11	8.192E-11	5.531E-03	4.637E-13	9.415E-11			
1.194E+00	6.315E-11	7.871E-11	4.307E-03	4.080E-13	1.063E-10			
1.054E+00	5.453E-11	6.968E-11	3.355E-03	3.705E-13	1.202E-10			
9.301E-01	4.677E-11	6.197E-11	2.613E-03	3.480E-13	1.360E-10			
8.209E-01	4.075E-11	5.634E-11	2.035E-03	3.377E-13	1.539E-10			
7.244E-01	3.592E-11	5.216E-11	1.585E-03	3.379E-13	1.743E-10			
6.393E-01	2.844E-11	4.562E-11	1.234E-03	3.476E-13	1.974E-10			
5.642E-01	2.782E-11	4.650E-11	9.611E-04	3.661E-13	2.236E-10			
4.979E-01	2.699E-11	4.797E-11	7.485E-04	3.927E-13	2.533E-10			
4.394E-01	2.504E-11	4.957E-11	5.830E-04	4.274E-13	2.871E-10			
3.877E-01	2.682E-11	5.750E-11	4.540E-04	4.710E-13	3.253E-10			
3.422E-01	2.670E-11	6.879E-11	3.536E-04	5.227E-13	3.686E-10			
3.020E-01	2.804E-11	9.309E-11	2.754E-04	5.831E-13	4.177E-10			
2.665E-01	3.821E-11	1.504E-10	2.145E-04	6.532E-13	4.734E-10			
2.352E-01	3.585E-11	2.090E-10	1.670E-04	7.336E-13	5.365E-10			
2.075E-01	1.700E-11	1.769E-10	1.301E-04	8.262E-13	6.081E-10			
1.832E-01	1.121E-11	1.142E-10	1.013E-04	9.317E-13	6.891E-10			
1.616E-01	9.773E-12	7.795E-11	7.889E-05	1.052E-12	7.810E-10			
1.426E-01	8.753E-12	5.982E-11	6.144E-05	1.188E-12	8.847E-10			
1.259E-01	6.867E-12	4.940E-11	4.785E-05	1.344E-12	1.002E-09			
1.111E-01	6.706E-12	4.474E-11	3.727E-05	1.521E-12	1.136E-09			

* Read as 1.649×10^{1}

Table 9 Calculated response of solid state nuclear track detector.

Energy [MeV]	Response [Pits/n]	Energy [MeV]	Response [Pits/n]
1.00E-01 *	3.64E-04	3.44E+00	9.51E-04
2.00E-01	4.92E-04	3.52E+00	9.24E-04
3.50E-01	5.33E-04	3.80E+00	9.16E-04
4.35E-01	6.59E-04	4.00E+00	9.45E-04
5.00E-01	5.01E-04	4.27E+00	9.52E-04
6.00E-01	5.34E-04	5.00E+00	9.36E-04
8.00E-01	5.52E-04	6.00E+00	9.55E-04
1.00E+00	6.27E-04	6.30E+00	1.02E-03
1.22E+00	6.02E-04	7.00E+00	9.43E-04
1.32E+00	6.95E-04	7.75E+00	9.84E-04
1.65E+00	7.59E-04	8.00E+00	9.44E-04
2.00E+00	7.07E-04	1.00E+01	8.86E-04
2.08E+00	8.29E-04	1.20E+01	7.33E-04
2.35E+00	7.37E-04	1.50E+01	2.85E-04
2.82E+00	8.93E-04	1.60E+01	2.41E-04
2.94E+00	8.66E-04	1.88E+01	2.21E-04
3.00E+00	7.96E-04	2.00E+01	2.16E-04
3.21E+00	8.77E-04		

* Read as 1.00×10^{-1}

Table 10 Neutron spectra behind 25-cm thick concrete shield measured with BC501A detector for 43-MeV p-^{7}Li neutrons.

Upper Energy Boundary [eV]	Neutron Flux [n cm^{-2} lethargy^{-1} μC^{-1}], Error [%]					
	beam axis		20cm from axis		40cm from axis	
4.40E+07*	6.74E+03	10.3	1.03E+02	55.9	1.24E+01	20.5
4.30E+07	1.32E+04	6.3	1.86E+02	64.5	2.33E+01	21.9
4.20E+07	1.97E+04	4.6	3.22E+02	40.0	3.20E+01	17.4
4.10E+07	2.27E+04	4.7	4.61E+02	12.7	3.46E+01	8.1
4.00E+07	2.02E+04	5.3	5.04E+02	11.3	3.26E+01	9.4
3.90E+07	1.40E+04	6.0	4.15E+02	24.4	2.85E+01	17.6
3.80E+07	7.43E+03	6.0	2.74E+02	29.7	2.32E+01	17.6
3.70E+07	3.13E+03	5.8	1.73E+02	22.0	1.83E+01	10.5
3.60E+07	1.33E+03	12.9	1.30E+02	10.7	1.55E+01	6.0
3.50E+07	1.02E+03	17.8	1.19E+02	11.2	1.46E+01	7.0
3.40E+07	1.27E+03	13.8	1.17E+02	10.6	1.45E+01	6.9
3.30E+07	1.61E+03	11.4	1.16E+02	9.2	1.45E+01	6.3
3.20E+07	1.88E+03	10.4	1.14E+02	8.3	1.44E+01	6.1
3.10E+07	2.05E+03	9.5	1.13E+02	8.5	1.42E+01	6.3
3.00E+07	2.15E+03	8.8	1.11E+02	9.6	1.39E+01	6.8
2.90E+07	2.17E+03	9.1	1.08E+02	11.3	1.37E+01	7.7
2.80E+07	2.13E+03	11.2	1.05E+02	13.7	1.34E+01	9.0
2.70E+07	2.04E+03	15.0	1.02E+02	16.5	1.32E+01	10.5
2.60E+07	1.93E+03	19.5	9.92E+01	18.6	1.31E+01	11.6
2.50E+07	1.82E+03	22.3	9.72E+01	19.3	1.30E+01	11.7
2.40E+07	1.73E+03	22.1	9.57E+01	17.8	1.30E+01	10.8
2.30E+07	1.67E+03	17.9	9.45E+01	14.1	1.30E+01	8.8
2.20E+07	1.64E+03	11.2	9.34E+01	8.9	1.31E+01	6.2
2.10E+07	1.64E+03	4.9	9.20E+01	4.8	1.31E+01	4.5
2.00E+07	1.65E+03	8.8	9.03E+01	6.7	1.30E+01	5.1
1.90E+07	1.63E+03	13.3	8.80E+01	9.3	1.29E+01	6.0
1.80E+07	1.55E+03	13.4	8.49E+01	9.3	1.25E+01	5.9
1.70E+07	1.42E+03	8.7	8.13E+01	7.1	1.21E+01	5.1
1.60E+07	1.27E+03	4.8	7.75E+01	5.2	1.17E+01	4.6
1.50E+07	1.16E+03	5.6	7.42E+01	4.9	1.13E+01	4.5
1.40E+07	1.11E+03	4.7	7.16E+01	5.7	1.11E+01	4.7
1.30E+07	1.09E+03	9.2	6.96E+01	8.0	1.10E+01	5.5
1.20E+07	1.05E+03	13.1	6.79E+01	9.9	1.10E+01	6.1
1.10E+07	9.85E+02	13.7	6.63E+01	10.4	1.10E+01	6.2
1.00E+07	9.11E+02	11.9	6.50E+01	8.7	1.11E+01	5.5
9.00E+06	8.46E+02	7.2	6.35E+01	4.5	1.13E+01	4.4
8.00E+06	7.56E+02	10.8	5.91E+01	14.9	1.11E+01	7.4
7.00E+06	6.76E+02	22.7	4.85E+01	38.7	9.77E+00	15.6
6.00E+06	6.94E+02	6.9				
5.00E+06	6.34E+02	43.1				
4.00E+06						

* Read as 4.40 x 10^7

Table 11 Neutron spectra behind 50-cm thick concrete shield measured with BC501A detector for 43-MeV p-^{7}Li neutrons.

Upper Energy Boundary [eV]	Neutron Flux [n cm^{-2} lethargy^{-1} μC^{-1}], beam axis	Error [%]	20cm from axis	Error [%]	40cm from axis	Error [%]
4.40E+07*	9.29E+02	10.9	7.64E+01	30.7	1.15E+01	20.5
4.30E+07	1.61E+03	6.5	1.39E+02	35.2	2.24E+01	21.3
4.20E+07	2.22E+03	4.6	2.22E+02	23.7	3.34E+01	15.5
4.10E+07	2.43E+03	4.7	2.96E+02	8.6	4.01E+01	7.0
4.00E+07	2.11E+03	5.2	3.16E+02	8.0	4.01E+01	7.7
3.90E+07	1.45E+03	5.7	2.66E+02	15.7	3.39E+01	14.2
3.80E+07	7.94E+02	5.5	1.79E+02	18.6	2.47E+01	15.8
3.70E+07	3.71E+02	5.3	1.07E+02	14.8	1.69E+01	10.7
3.60E+07	1.91E+02	11.8	7.06E+01	8.3	1.28E+01	6.3
3.50E+07	1.52E+02	14.6	5.84E+01	8.9	1.14E+01	8.1
3.40E+07	1.64E+02	12.0	5.55E+01	8.7	1.10E+01	7.9
3.30E+07	1.83E+02	10.7	5.46E+01	7.7	1.06E+01	7.2
3.20E+07	1.97E+02	10.6	5.36E+01	7.4	1.03E+01	6.9
3.10E+07	2.05E+02	10.3	5.23E+01	7.9	9.85E+00	7.2
3.00E+07	2.07E+02	9.9	5.07E+01	9.0	9.36E+00	8.1
2.90E+07	2.03E+02	10.5	4.91E+01	10.8	8.81E+00	9.6
2.80E+07	1.92E+02	13.3	4.75E+01	13.2	8.21E+00	12.1
2.70E+07	1.76E+02	18.8	4.60E+01	15.9	7.61E+00	15.1
2.60E+07	1.58E+02	25.5	4.44E+01	18.1	7.10E+00	17.8
2.50E+07	1.43E+02	30.7	4.27E+01	19.1	6.77E+00	19.0
2.40E+07	1.33E+02	30.7	4.06E+01	18.2	6.66E+00	17.5
2.30E+07	1.30E+02	24.8	3.83E+01	15.1	6.77E+00	13.6
2.20E+07	1.30E+02	14.7	3.58E+01	9.9	7.03E+00	8.3
2.10E+07	1.32E+02	5.3	3.31E+01	4.9	7.33E+00	4.7
2.00E+07	1.33E+02	11.2	3.06E+01	7.8	7.50E+00	5.9
1.90E+07	1.30E+02	18.1	2.84E+01	11.9	7.40E+00	7.7
1.80E+07	1.19E+02	18.9	2.67E+01	12.2	6.98E+00	7.7
1.70E+07	1.03E+02	12.5	2.54E+01	8.9	6.34E+00	6.3
1.60E+07	8.75E+01	5.4	2.42E+01	5.8	5.75E+00	5.0
1.50E+07	7.84E+01	7.1	2.31E+01	5.2	5.40E+00	4.8
1.40E+07	7.75E+01	5.1	2.20E+01	6.8	5.34E+00	5.5
1.30E+07	8.04E+01	12.9	2.09E+01	10.7	5.43E+00	7.3
1.20E+07	8.14E+01	18.2	1.99E+01	14.0	5.51E+00	8.7
1.10E+07	7.84E+01	18.4	1.92E+01	14.7	5.51E+00	8.8
1.00E+07	7.37E+01	15.7	1.90E+01	11.9	5.41E+00	7.5
9.00E+06	6.80E+01	8.8	1.94E+01	4.6	5.06E+00	4.5
8.00E+06	5.69E+01	15.0	2.02E+01	18.6	4.09E+00	14.8
7.00E+06	4.82E+01	38.4	1.95E+01	42.0		
6.00E+06	5.01E+01	28.5				
5.00E+06	3.20E+01	73.7				
4.00E+06						

* Read as 4.40 x 10^7

Table 12 Neutron spectra behind 100- and150-cm thick concrete shields measured with BC501A detector for 43-MeV p-^{7}Li neutrons.

Upper Energy Boundary [eV]	Neutron Flux [n cm^{-2} lethargy^{-1} μC^{-1}] , 100 cm thick	Error [%]	150 cm thick	Error [%]
4.40E+07*	7.98E+00	7.7	2.03E-01	11.7
4.30E+07	1.66E+01	5.7	3.91E-01	8.8
4.20E+07	2.74E+01	4.8	6.25E-01	7.2
4.10E+07	3.59E+01	4.5	8.16E-01	5.8
4.00E+07	3.73E+01	4.9	8.65E-01	4.9
3.90E+07	3.10E+01	5.9	7.47E-01	8.2
3.80E+07	2.13E+01	6.6	5.40E-01	15.6
3.70E+07	1.31E+01	5.8	3.57E-01	21.2
3.60E+07	8.37E+00	5.0	2.51E-01	15.7
3.50E+07	6.42E+00	7.4	2.11E-01	7.0
3.40E+07	5.78E+00	8.0	2.00E-01	13.7
3.30E+07	5.53E+00	7.6	1.93E-01	16.3
3.20E+07	5.31E+00	7.6	1.85E-01	15.6
3.10E+07	5.06E+00	7.7	1.74E-01	14.4
3.00E+07	4.80E+00	7.8	1.63E-01	13.8
2.90E+07	4.54E+00	8.7	1.53E-01	14.6
2.80E+07	4.29E+00	11.0	1.46E-01	16.5
2.70E+07	4.04E+00	15.0	1.41E-01	19.0
2.60E+07	3.75E+00	19.9	1.36E-01	21.3
2.50E+07	3.40E+00	23.7	1.29E-01	22.6
2.40E+07	3.03E+00	24.8	1.18E-01	22.2
2.30E+07	2.68E+00	21.9	1.05E-01	19.4
2.20E+07	2.38E+00	14.7	8.81E-02	13.7
2.10E+07	2.17E+00	5.7	7.13E-02	6.6
2.00E+07	2.03E+00	12.9	5.71E-02	12.8
1.90E+07	1.93E+00	21.3	4.81E-02	22.4
1.80E+07	1.85E+00	21.2	4.53E-02	22.4
1.70E+07	1.75E+00	12.6	4.67E-02	14.6
1.60E+07	1.65E+00	5.7	4.87E-02	8.2
1.50E+07	1.55E+00	7.2	4.83E-02	6.7
1.40E+07	1.46E+00	5.1	4.50E-02	9.8
1.30E+07	1.39E+00	13.3	4.06E-02	18.0
1.20E+07	1.33E+00	20.2	3.71E-02	25.5
1.10E+07	1.30E+00	20.4	3.59E-02	27.1
1.00E+07	1.31E+00	16.2	3.78E-02	20.4
9.00E+06	1.38E+00	8.2	4.51E-02	5.2
8.00E+06	1.44E+00	11.4	5.83E-02	22.8
7.00E+06	1.52E+00	22.7	6.87E-02	42.2
6.00E+06	1.66E+00	16.3	6.31E-02	54.9
5.00E+06	1.57E+00	27.5		
4.00E+06				

* Read as 4.40 x 10^7

Detector was placed on the beam axis.

Table 13 Neutron spectra behind 25-cm thick concrete shield measured with BC501A detector for 68-MeV p-^{7}Li neutrons.

Upper Energy Boundary [eV]	Neutron Flux [n cm^{-2} lethargy^{-1} μC^{-1}], Error [%]					
	beam axis		20cm from axis		40cm from axis	
7.00E+07*	1.60E+04	4.8	1.08E+02	11.6	5.04E+00	13.8
6.80E+07	3.24E+04	4.7	2.58E+02	14.6	9.94E+00	21.6
6.60E+07	4.58E+04	4.5	4.95E+02	11.3	2.36E+01	13.7
6.40E+07	4.66E+04	4.4	5.34E+02	11.6	3.37E+01	11.6
6.20E+07	3.48E+04	4.7	3.76E+02	15.8	2.14E+01	18.9
6.00E+07	1.95E+04	5.1	1.77E+02	15.8	1.35E+01	14.1
5.80E+07	9.14E+03	4.9	1.23E+02	13.6	1.41E+01	9.0
5.60E+07	5.44E+03	5.9	1.51E+02	9.6	1.52E+01	7.4
5.40E+07	5.55E+03	6.3	1.75E+02	6.2	1.58E+01	5.7
5.20E+07	6.56E+03	5.5	1.89E+02	5.7	1.67E+01	5.4
5.00E+07	7.05E+03	5.2	2.00E+02	5.9	1.86E+01	5.5
4.80E+07	6.74E+03	5.2	2.14E+02	6.3	2.08E+01	5.8
4.60E+07	5.92E+03	5.2	2.24E+02	6.2	2.20E+01	5.8
4.40E+07	5.28E+03	5.3	2.26E+02	6.0	2.22E+01	5.5
4.30E+07	4.94E+03	5.5	2.26E+02	5.8	2.23E+01	5.3
4.20E+07	4.69E+03	5.7	2.25E+02	5.7	2.24E+01	5.1
4.10E+07	4.53E+03	5.9	2.25E+02	5.9	2.29E+01	5.3
4.00E+07	4.42E+03	6.3	2.25E+02	6.4	2.35E+01	5.7
3.90E+07	4.35E+03	6.7	2.25E+02	6.8	2.43E+01	5.9
3.80E+07	4.27E+03	6.9	2.27E+02	6.9	2.53E+01	5.8
3.70E+07	4.17E+03	7.1	2.28E+02	6.6	2.64E+01	5.7
3.60E+07	4.02E+03	7.3	2.30E+02	6.3	2.74E+01	5.3
3.50E+07	3.83E+03	7.6	2.31E+02	5.9	2.83E+01	5.2
3.40E+07	3.63E+03	7.8	2.30E+02	5.8	2.88E+01	5.3
3.30E+07	3.44E+03	8.1	2.28E+02	6.2	2.87E+01	5.7
3.20E+07	3.31E+03	8.2	2.23E+02	6.7	2.81E+01	6.3
3.10E+07	3.24E+03	8.2	2.16E+02	6.9	2.72E+01	6.3
3.00E+07	3.23E+03	8.3	2.08E+02	6.3	2.63E+01	5.7
2.90E+07	3.24E+03	8.7	2.01E+02	5.7	2.57E+01	5.1
2.80E+07	3.21E+03	9.6	1.94E+02	5.7	2.53E+01	5.2
2.70E+07	3.10E+03	10.8	1.87E+02	7.0	2.52E+01	6.4
2.60E+07	2.90E+03	12.3	1.79E+02	9.3	2.51E+01	8.8
2.50E+07	2.63E+03	13.6	1.70E+02	11.0	2.48E+01	10.3
2.40E+07	2.31E+03	14.0	1.60E+02	10.9	2.42E+01	9.9
2.30E+07	2.00E+03	12.8	1.50E+02	9.2	2.32E+01	8.2
2.20E+07	1.69E+03	9.7	1.41E+02	6.9	2.20E+01	6.1
2.10E+07	1.40E+03	6.0	1.32E+02	5.1	2.04E+01	4.6
2.00E+07	1.14E+03	10.9	1.24E+02	7.0	1.88E+01	6.1
1.90E+07	9.22E+02	17.9	1.15E+02	11.0	1.74E+01	9.5
1.80E+07	7.64E+02	21.0	1.06E+02	12.7	1.66E+01	10.6
1.70E+07	6.72E+02	17.7	9.82E+01	9.7	1.62E+01	7.3
1.60E+07	6.32E+02	11.7	9.11E+01	6.8	1.59E+01	5.2
1.50E+07	6.17E+02	8.4	8.51E+01	8.3	1.55E+01	6.6
1.40E+07	5.99E+02	10.0	8.11E+01	5.4	1.49E+01	4.8
1.30E+07	5.71E+02	15.9	7.98E+01	7.2	1.44E+01	5.9
1.20E+07	5.41E+02	21.1	7.99E+01	8.8	1.44E+01	7.3
1.10E+07	5.22E+02	22.1	8.00E+01	7.7	1.46E+01	6.4
1.00E+07	5.21E+02	17.5	7.94E+01	6.3	1.47E+01	5.4
9.00E+06	5.35E+02	5.7	7.89E+01	5.5	1.48E+01	4.9
8.00E+06	5.49E+02	28.1	8.07E+01	4.9	1.54E+01	4.5
7.00E+06	5.21E+02	64.0				
6.00E+06						

* Read as 7.00 x 10^7

Table 14 Neutron spectra behind 50-cm thick concrete shield measured with BC501A detector for 68-MeV p-^{7}Li neutrons.

Upper Energy Boundary [eV]	Neutron Flux [n cm^{-2} lethargy^{-1} μC^{-1}], beam axis	Error [%]	20cm from axis	Error [%]	40cm from axis	Error [%]
7.00E+07*	3.12E+03	5.0	1.77E+02	6.4	8.31E+00	10.1
6.80E+07	6.41E+03	4.8	4.78E+02	10.0	2.99E+01	13.7
6.60E+07	9.06E+03	4.5	7.98E+02	7.0	5.90E+01	8.2
6.40E+07	9.24E+03	4.4	7.49E+02	6.8	6.74E+01	7.2
6.20E+07	6.95E+03	4.8	4.57E+02	12.3	5.14E+01	11.6
6.00E+07	3.92E+03	5.2	2.16E+02	15.6	3.00E+01	12.5
5.80E+07	1.79E+03	5.1	1.28E+02	9.5	2.07E+01	7.2
5.60E+07	9.30E+02	6.3	1.32E+02	12.0	2.10E+01	8.9
5.40E+07	8.46E+02	7.6	1.53E+02	7.7	2.28E+01	6.5
5.20E+07	9.85E+02	6.3	1.67E+02	6.2	2.40E+01	5.6
5.00E+07	1.07E+03	5.6	1.74E+02	6.2	2.49E+01	5.7
4.80E+07	1.05E+03	5.3	1.75E+02	6.3	2.54E+01	5.9
4.60E+07	9.53E+02	5.2	1.73E+02	6.1	2.58E+01	5.7
4.40E+07	8.57E+02	5.4	1.70E+02	6.1	2.61E+01	5.5
4.30E+07	7.93E+02	5.5	1.66E+02	6.1	2.63E+01	5.4
4.20E+07	7.34E+02	5.8	1.63E+02	6.3	2.67E+01	5.5
4.10E+07	6.82E+02	6.3	1.59E+02	6.8	2.71E+01	5.7
4.00E+07	6.38E+02	6.9	1.56E+02	7.4	2.75E+01	6.0
3.90E+07	5.98E+02	7.6	1.52E+02	7.9	2.79E+01	6.3
3.80E+07	5.63E+02	8.2	1.48E+02	8.2	2.81E+01	6.3
3.70E+07	5.31E+02	8.8	1.44E+02	8.2	2.81E+01	6.3
3.60E+07	5.00E+02	9.3	1.39E+02	7.9	2.78E+01	6.2
3.50E+07	4.71E+02	9.8	1.34E+02	7.7	2.72E+01	6.1
3.40E+07	4.46E+02	10.2	1.28E+02	7.5	2.64E+01	6.1
3.30E+07	4.27E+02	10.5	1.21E+02	7.6	2.55E+01	6.3
3.20E+07	4.16E+02	10.5	1.14E+02	7.7	2.45E+01	6.3
3.10E+07	4.12E+02	10.6	1.07E+02	7.8	2.35E+01	6.3
3.00E+07	4.13E+02	10.7	1.01E+02	7.6	2.25E+01	6.1
2.90E+07	4.14E+02	11.1	9.59E+01	7.4	2.14E+01	6.1
2.80E+07	4.11E+02	11.8	9.17E+01	7.7	2.04E+01	6.6
2.70E+07	3.99E+02	12.8	8.76E+01	8.5	1.94E+01	7.7
2.60E+07	3.78E+02	13.6	8.33E+01	9.5	1.84E+01	9.0
2.50E+07	3.48E+02	14.2	7.86E+01	10.3	1.75E+01	10.0
2.40E+07	3.11E+02	13.9	7.37E+01	10.3	1.65E+01	9.9
2.30E+07	2.70E+02	12.5	6.89E+01	9.2	1.55E+01	8.7
2.20E+07	2.27E+02	10.0	6.43E+01	7.3	1.45E+01	6.7
2.10E+07	1.85E+02	7.3	6.00E+01	5.6	1.36E+01	4.9
2.00E+07	1.47E+02	10.5	5.61E+01	8.1	1.27E+01	6.8
1.90E+07	1.16E+02	17.1	5.24E+01	11.1	1.19E+01	9.4
1.80E+07	9.45E+01	21.2	4.85E+01	12.3	1.10E+01	10.0
1.70E+07	8.22E+01	20.8	4.44E+01	10.8	1.03E+01	8.1
1.60E+07	7.69E+01	17.6	4.05E+01	7.6	9.65E+00	5.5
1.50E+07	7.57E+01	15.3	3.75E+01	6.8	9.05E+00	5.5
1.40E+07	7.64E+01	15.7	3.57E+01	5.3	8.57E+00	4.7
1.30E+07	7.82E+01	18.4	3.45E+01	7.3	8.26E+00	6.4
1.20E+07	8.13E+01	20.4	3.34E+01	8.8	8.13E+00	7.8
1.10E+07	8.55E+01	18.8	3.27E+01	8.8	8.11E+00	7.7
1.00E+07	9.06E+01	12.0	3.28E+01	7.7	8.22E+00	6.7
9.00E+06	9.56E+01	8.4	3.38E+01	5.6	8.55E+00	5.1
8.00E+06	9.74E+01	29.9	3.22E+01	6.8	8.88E+00	6.5
7.00E+06	9.01E+01	55.4				
6.00E+06						

* Read as 7.00 x 10^7

Table 15 Neutron spectra behind 100-, 150- and 200-cm thick concrete shields measured with BC501A detector for 68-MeV p-^{7}Li neutrons.

Upper Energy Boundary [eV]	Neutron Flux [n cm^{-2} lethargy^{-1} μC^{-1}], 100 cm thick	Error [%]	150 cm thick	Error [%]	200 cm thick	Error [%]
7.00E+07*	1.41E+02	5.5	4.22E+00	6.8	5.35E-01	9.6
6.80E+07	2.83E+02	5.2	9.86E+00	5.8	1.24E+00	7.5
6.60E+07	3.99E+02	4.6	1.68E+01	4.7	2.10E+00	5.2
6.40E+07	4.10E+02	4.5	2.07E+01	4.6	2.62E+00	5.0
6.20E+07	3.14E+02	5.1	1.84E+01	5.0	2.42E+00	6.1
6.00E+07	1.82E+02	5.8	1.21E+01	5.3	1.71E+00	6.5
5.80E+07	8.64E+01	5.5	6.54E+00	5.0	1.04E+00	5.5
5.60E+07	4.69E+01	7.7	4.04E+00	6.5	6.85E-01	7.7
5.40E+07	4.31E+01	9.1	3.65E+00	6.9	5.88E-01	8.6
5.20E+07	4.97E+01	7.3	3.85E+00	6.3	5.84E-01	7.8
5.00E+07	5.39E+01	6.5	3.88E+00	6.3	5.82E-01	8.1
4.80E+07	5.24E+01	6.4	3.55E+00	6.9	5.55E-01	8.8
4.60E+07	4.66E+01	6.5	2.96E+00	7.5	4.99E-01	9.3
4.40E+07	4.15E+01	6.8	2.51E+00	8.2	4.54E-01	9.6
4.30E+07	3.84E+01	7.2	2.29E+00	8.7	4.32E-01	9.9
4.20E+07	3.60E+01	7.7	2.15E+00	9.3	4.21E-01	10.5
4.10E+07	3.42E+01	8.5	2.11E+00	10.2	4.20E-01	11.5
4.00E+07	3.30E+01	9.5	2.12E+00	11.2	4.26E-01	12.5
3.90E+07	3.20E+01	10.2	2.14E+00	11.7	4.32E-01	13.1
3.80E+07	3.10E+01	10.7	2.15E+00	11.9	4.34E-01	13.4
3.70E+07	2.98E+01	11.0	2.12E+00	11.7	4.25E-01	13.2
3.60E+07	2.82E+01	11.3	2.03E+00	11.5	4.04E-01	12.9
3.50E+07	2.62E+01	11.6	1.89E+00	11.3	3.74E-01	12.7
3.40E+07	2.39E+01	12.2	1.72E+00	11.6	3.38E-01	12.8
3.30E+07	2.18E+01	12.8	1.55E+00	12.4	3.02E-01	13.3
3.20E+07	2.02E+01	13.0	1.42E+00	13.1	2.72E-01	14.1
3.10E+07	1.93E+01	13.0	1.34E+00	13.1	2.50E-01	14.3
3.00E+07	1.91E+01	12.6	1.34E+00	12.2	2.36E-01	13.7
2.90E+07	1.93E+01	12.5	1.37E+00	11.4	2.25E-01	13.2
2.80E+07	1.93E+01	12.9	1.40E+00	11.6	2.13E-01	13.9
2.70E+07	1.90E+01	13.9	1.38E+00	13.0	2.00E-01	15.7
2.60E+07	1.80E+01	15.2	1.31E+00	15.2	1.87E-01	18.2
2.50E+07	1.66E+01	16.5	1.21E+00	17.3	1.76E-01	20.1
2.40E+07	1.49E+01	16.7	1.10E+00	17.6	1.65E-01	20.0
2.30E+07	1.32E+01	15.1	1.01E+00	15.7	1.54E-01	17.5
2.20E+07	1.16E+01	11.9	9.19E-01	11.7	1.42E-01	13.5
2.10E+07	9.98E+00	8.3	8.30E-01	7.5	1.30E-01	9.5
2.00E+07	8.44E+00	14.8	7.35E-01	13.8	1.19E-01	16.7
1.90E+07	7.07E+00	22.8	6.32E-01	22.1	1.10E-01	24.5
1.80E+07	6.04E+00	26.7	5.32E-01	26.9	1.02E-01	27.6
1.70E+07	5.50E+00	23.5	4.61E-01	23.7	9.63E-02	23.8
1.60E+07	5.42E+00	16.2	4.34E-01	13.7	9.14E-02	15.3
1.50E+07	5.63E+00	10.6	4.47E-01	11.1	8.72E-02	12.0
1.40E+07	5.87E+00	9.9	4.73E-01	6.6	8.51E-02	7.7
1.30E+07	6.05E+00	12.6	4.92E-01	11.4	8.61E-02	12.0
1.20E+07	6.20E+00	15.0	4.98E-01	14.3	8.88E-02	14.1
1.10E+07	6.40E+00	14.9	5.01E-01	14.0	9.01E-02	13.7
1.00E+07	6.73E+00	11.6	5.14E-01	11.4	9.11E-02	11.5
9.00E+06	7.12E+00	5.5	5.51E-01	7.1	9.62E-02	7.3
8.00E+06	7.19E+00	16.8	5.92E-01	10.3	1.04E-01	8.8
7.00E+06	6.38E+00	38.1	5.73E-01	28.0	1.10E-01	11.9
6.00E+06						

* Read as 7.00 x 10^7

Detector was placed on the beam axis.

Table 16 Counting rates behind the concrete shields measured with Boner ball counter for 43 MeV p-^{7}Li neutrons.

Moderator Thickness	Reaction Rate [counts μC^{-1}]			
	25 cm thick[a]	50 cm thick	100 cm thick	150 cm thick
Bare	5.20E+03 [b]	1.32E+03	6.45E+01	2.73E+00
1.5 cm	5.98E+03	1.25E+03	4.84E+01	2.28E+00
1.5 cm + Cd	-	-	-	-
3.0 cm	8.94E+03	1.59E+03	6.62E+01	2.89E+00
5.0 cm	1.19E+04	1.90E+03	5.27E+01	3.02E+00
9.0 cm	1.11E+04	1.62E+03	5.27E+01	2.36E+00

a Concrete shield thickness
b Read as 5.20 x 10^{3}

Table 17 Counting rates behind the concrete shields measured with Bonner ball counter for 68 MeV p-^{7}Li neutrons.

Moderator Thickness	Reaction Rate [counts μC^{-1}]			
	25 cm thick[a]	50 cm thick	100 cm thick	150 cm thick
Bare	-	2.04E+03 [b]	2.74E+02	1.83E+01
1.5 cm	-	2.16E+03	-	-
1.5 cm + Cd	-	-	1.44E+02	1.06E+01
3.0 cm	-	3.04E+03	3.15E+02	2.42E+01
5.0 cm	-	3.72E+03	3.62E+02	2.86E+01
9.0 cm	-	3.25E+03	3.08E+02	2.46E+01

a Concrete shield thickness
b Read as 2.04 x 10^{3}

Table 18 Neutron spectra behind the concrete shields measured with Bonner ball counter for 43-MeV p-^{7}Li neutrons.

Upper Energy Boundary [eV]	Neutron Flux [n cm^{-2} lethargy^{-1} μC^{-1}]			
	25cm thick [a]	50cm thick	100cm thick	150cm thick
4.50E+07 [b]	5.50E+03	7.25E+02	1.64E+01	4.23E-01
3.50E+07	1.07E+03	1.56E+02	6.27E+00	2.29E-01
2.75E+07	1.11E+03	1.32E+02	3.57E+00	1.50E-01
2.25E+07	8.81E+02	9.57E+01	2.49E+00	1.63E-01
1.75E+07	5.74E+02	6.53E+01	1.64E+00	5.82E-02
1.35E+07	4.01E+02	4.63E+01	1.37E+00	4.17E-02
1.00E+07	2.94E+02	4.20E+01	1.17E+00	3.87E-02
6.70E+06	2.54E+02	3.66E+01	1.65E+00	9.71E-02
4.49E+06	2.00E+02	3.34E+01	1.11E+00	5.72E-02
3.01E+06	2.43E+02	4.35E+01	1.95E+00	9.17E-02
2.02E+06	1.88E+02	3.18E+01	1.33E+00	5.96E-02
1.35E+06	1.53E+02	1.75E+01	4.83E-01	3.53E-02
9.07E+05	1.59E+02	2.61E+01	7.89E-01	3.74E-02
4.98E+05	9.49E+01	1.39E+01	4.29E-01	1.65E-02
2.24E+05	8.16E+01	1.16E+01	2.06E-01	1.42E-02
8.65E+04	6.46E+01	8.35E+00	2.93E-01	1.01E-02
1.50E+04	4.64E+01	7.13E+00	2.64E-01	1.16E-02
3.35E+03	5.41E+01	8.59E+00	2.63E-01	1.78E-02
4.54E+02	5.61E+01	1.09E+01	5.14E-01	2.24E-02
2.26E+01	4.45E+01	1.07E+01	1.94E-01	1.45E-02
5.04E+00	3.38E+01	1.17E+01	5.96E-01	2.94E-02
1.12E+00	3.77E+01	1.40E+01	7.43E-01	2.22E-02
4.14E-01	2.17E+01	4.90E+00	2.47E-01	1.08E-02
1.00E-04				

a Concrete shield thickness
b Read as 4.50 x 10^7

Table 19 Neutron spectra behind the concrete shields measured with Bonner ball counter for 68-MeV p-^{7}Li neutrons.

Upper Energy Boundary [eV]	Neutron Flux [n cm^{-2} lethargy^{-1} μC^{-1}]		
	50cm thick [a]	100cm thick	150cm thick
8.00E+07[b]	6.85E+02	1.67E+01	5.78E-01
6.50E+07	2.15E+03	8.79E+01	7.23E+00
5.50E+07	4.82E+02	2.08E+01	1.52E+00
4.50E+07	3.07E+02	1.95E+01	1.50E+00
3.50E+07	2.13E+02	6.42E+00	8.23E-01
2.75E+07	1.30E+02	9.62E+00	8.43E-01
2.25E+07	8.87E+01	1.32E+01	1.74E-01
1.75E+07	6.50E+01	5.11E+00	2.95E-01
1.35E+07	5.28E+01	5.13E+00	2.52E-01
1.00E+07	5.30E+01	4.47E+00	2.17E-01
6.70E+06	6.30E+01	7.35E+00	9.47E-01
4.49E+06	6.10E+01	9.71E+00	7.83E-01
3.01E+06	8.68E+01	1.19E+01	8.97E-01
2.02E+06	5.92E+01	1.02E+01	9.92E-01
1.35E+06	4.13E+01	5.90E+00	5.58E-01
9.07E+05	5.76E+01	7.62E+00	5.23E-01
4.98E+05	3.25E+01	4.20E+00	4.41E-01
2.24E+05	2.65E+01	4.17E+00	2.67E-01
8.65E+04	1.83E+01	1.91E+00	5.15E-02
1.50E+04	1.77E+01	1.07E+00	7.83E-02
3.35E+03	1.69E+01	8.00E-01	1.34E-01
4.54E+02	1.91E+01	9.29E-01	9.11E-02
2.26E+01	1.81E+01	7.61E-01	7.31E-02
5.04E+00	1.55E+01	1.21E+00	6.62E-02
1.12E+00	1.64E+01	2.42E+00	4.13E-02
4.14E-01	8.26E+00	1.29E+00	9.93E-02
1.00E-04			

* Read as 8.00 x 10^{7}

Table 20 Fission rates of ^{238}U and ^{232}Th fission counter measured behind the concrete shield for 43-MeV p-^{7}Li neutrons.

Thickness Z[a] [cm]	Position R[b] [cm]	^{238}U Fission Rate [barn cm^{-2} μC^{-1}]	^{238}U Error [%]	^{232}Th Fission Rate [barn cm^{-2} μC^{-1}]	^{232}Th Error [%]
0	0	7.28E+04 [c]	0.4	3.07E+04	0.6
25	0	1.15E+04	1.4	4.32E+03	4.8
50	0	1.26E+03	5.6	5.23E+02	4.9
100	0	1.98E+01	8.0	7.80E+00	24.0
150	0	1.72E+00	17.0		
0	20	3.24E+02	6.4	6.24E+01	16.0
25	20	4.78E+02	15.0	1.48E+02	12.0
50	20	1.90E+02	8.4	7.58E+01	8.8
100	20	1.37E+01	17.0	5.73E+00	27.0
150	20	1.33E+00	20.0		

a Thichness of concrete shields
b Distance from the beam axis
c Read as 7.28 x 10^4

Table 21 Fission rates of ^{238}U and ^{232}Th fission counter measured behind the concrete shield for 68-MeV p-^{7}Li neutrons.

Thickness Z[a] [cm]	Position R[b] [cm]	^{238}U Fission Rate [barn cm^{-2} μC^{-1}]	^{238}U Error [%]	^{232}Th Fission Rate [barn cm^{-2} μC^{-1}]	^{232}Th Error [%]
0	0	1.18E+05 [c]	0.4	5.71E+04	0.5
25	0	2.37E+04	1.7	1.41E+04	2.2
50	0	4.63E+03	1.1	2.43E+03	1.4
100	0	1.72E+02	4.8	9.23E+01	6.4
150	0	9.47E+00	7.5	4.93E+00	10.0
25	20	1.28E+03	3.9	2.82E+02	8.1
50	20	7.82E+02	1.9	1.96E+02	3.7
100	20	8.30E+01	3.3	3.86E+01	4.7
150	20	7.41E+00	6.7	3.46E+00	9.5

a Thichness of concrete shields
b Distance from the beam axis
c Read as 1.18 x 10^5

Table 22 Differences of reaction rate of ^{7}LiF and ^{nat}LiF TLDs measured inside the150- and 200-cm thick concrete shields for 43- and 68-MeV p-^{7}Li neutrons, respectively.

	43 MeV		68 MeV	
Depth[a] [cm]	Reaction Rate Difference [^{60}Co-eq. R μC^{-1}]	Error [%]	Reaction Rate Difference [^{60}Co-eq. R μC^{-1}]	Error [%]
0	1.99E-05[b]	77.	3.16E-05	88.
25	4.67E-05	11.	6.57E-05	20.
50	9.14E-06	15.	2.46E-05	11.
75	1.72E-06	14.	6.62E-06	10.
100	3.48E-07	16.	1.66E-06	8.8
125	6.72E-08	60.	4.57E-07	12.
150	-	-	6.67E-08	22.

a Depth of the concrete shield where detectors were placed
b Read as 1.99 x 10^{-5}

Table 23 Reaction rate of solid state nuclear track detector measured inside the 150- and 200-cm thick concrete shield for 43- and 68-MeV p-^{7}Li neutrons, respectively.

	43 MeV		68 MeV	
Depth[a] [cm]	Reaction Rate Difference [^{60}Co-eq. R μC^{-1}]	Error [%]	Reaction Rate Difference [^{60}Co-eq. R μC^{-1}]	Error [%]
25	4.50E+00[b]	5.5	9.15E+00	5.5
50	4.27E-01	7.3	1.56E+00	6.6
75	4.72E-02	17.	3.12E-01	11.
100	4.50E-03	33.	5.50E-02	10.
125	1.53E-03	55.	1.75E-02	16.
150	-	-	4.19E-03	28.

a Depth of the concrete shield where detectors were placed
b Read as 4.50 x 10^{-5}

Table 24 Neutron dose-equivalent behind the concrete shield measured with a rem counter (Fuji Co. Ltd.).

43 MeV			68 MeV		
Shield Thickness [cm]	Dose Equivalent [μSv μC^{-1}]	Error [%]	Shield Thickness [cm]	Dose Equivalent [μSv μC^{-1}]	Error [%]
0	4.23E+00*	0.52	0	4.58E+00	0.45
25	5.68E-01	0.95	25	6.85E-01	0.36
50	4.63E-02	0.23	50	1.60E-01	0.70
100	1.97E-03	0.28	100	1.00E-02	1.4
150	6.78E-05	3.1	150	7.89E-04	1.5
			200	8.91E-05	4.5

* Read as 4.23 x 10^0

Table 25 Neutron dose-equivalent behind the concrete shields estimated by measured neutron spectra of BC501A(>10 MeV) and Bonner ball (<10 MeV).

43 MeV		68 MeV	
Shield Thickness [cm]	Dose Equivalent [μSv μC^{-1}]	Shield Thickness [cm]	Dose Equivalent [μSv μC^{-1}]
0	2.15E+01*	0	2.99E+01
25	2.51E+00	25	-
50	2.69E-01	50	1.17E+01
100	5.19E-03	100	5.19E-02
150	1.74E-04	150	3.27E-03
		200	-

* Read as 2.15 x 10^1